Article:
Mahian, O, Kianifara, A, Heris, SZ et al. (3 more authors) (2017) Nanofluids Effects on the Evaporation Rate in a Solar Still Equipped with a Heat Exchanger. Nano Energy, 36. pp. 134-155. ISSN 2211-2855

https://doi.org/10.1016/j.nanoen.2017.04.025

Nanofluids Effects on the Evaporation Rate in a Solar Still Equipped with a Heat Exchanger

Omid Mahian, Ali Kianifar, Saeed Zeinali Heris, Dongsheng Wen, Ahmet Z. Sahin, Somchai Wongwises

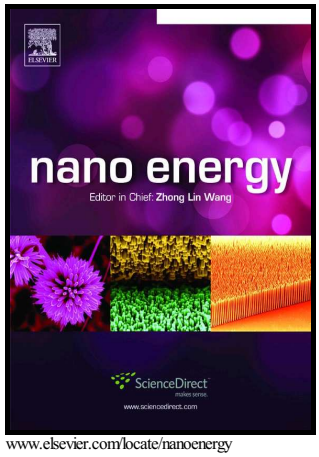

www.elsevier.com/locate/nanoenergy

PII: S2211-2855(17)30226-4
DOI: http://dx.doi.org/10.1016/j.nanoen.2017.04.025
Reference: NANOEN1905

To appear in: *Nano Energy*

Received date: 21 February 2017
Revised date: 14 April 2017
Accepted date: 15 April 2017

Cite this article as: Omid Mahian, Ali Kianifar, Saeed Zeinali Heris, Dongsheng Wen, Ahmet Z. Sahin and Somchai Wongwises, Nanofluids Effects on the Evaporation Rate in a Solar Still Equipped with a Heat Exchanger, *Nano Energy*, http://dx.doi.org/10.1016/j.nanoen.2017.04.025

Nanofluids Effects on the Evaporation Rate in a Solar Still Equipped with a Heat Exchanger

Omid Mahian[a*], Ali Kianifar[a], Saeed Zeinali Heris[b], Dongsheng Wen[c,d], Ahmet Z. Sahin[e], Somchai Wongwises[f]

[a]Department of Mechanical Engineering, Ferdowsi University of Mashhad, Iran

[b]Faculty of Chemical and Petroleum Engineering, University of Tabriz, Tabriz, Iran

[c]Laboratory of Fundamental Science on Ergonomics and Environmental Control, School of Aeronautic Science and Engineering, Beihang University, Beijing 100191, PR China

[d]School of Chemical and Process Engineering, University of Leeds, Leeds LS2 9JT, UK

[e]Mechanical Engineering Department, King Fahd University of Petroleum & Minerals (KFUPM), Dhahran 31261, Saudi Arabia

[f]Fluid Mechanics, Thermal Engineering and Multiphase Flow Research Laboratory(FUTURE Lab), Department of Mechanical Engineering, King Mongkut's University of Technology Thonburi, 126 Pracha-Utit Road, Thungkru, Bangmod, Bangmod, Bangkok 10140, Thailand

[*]Corresponding author. omid.mahian@gmail.com

Abstract

In this paper, the performance of a solar still equipped with a heat exchanger using nanofluids has been studied both experimentally and theoretically through three key parameters, i.e., freshwater yield, energy efficiency and exergy efficiency. First, experiments are performed on a set-up, which is mainly composed of two flat plate solar collectors connected in series, and a solar still equipped with a heat exchanger. After heated in the collectors, the nanofluid enters the heat exchanger installed in the solar still basin to exchange heat with brackish water. The research question is to know how much the effect of nanofluids on the evaporation rate inside the solar desalination system is. The experiments are conducted for different nanoparticle volume fractions, two sizes of nanoparticles (7 and 40 nm), two depths of water in the solar still basin (4 and 8 cm), and three mass flow rates of nanofluids during various weather conditions. It is found that the weather conditions (mainly the sun radiation intensity) have a dominant influence on the solar still performance. To discover the effects of nanofluids, a mathematical model is developed and validated by experimental data at given weather conditions. The results reveal that using the heat exchanger at temperatures lower than 60 ^{o}C is not advantageous and the corresponding yield is smaller than that of solar still without the heat exchanger; although in such a case, using

nanofluids as the working fluid in the heat exchanger can enhance the performance indices about 10%. At higher temperatures (e.g. 70 ^{o}C), the use of heat exchanger is beneficial; however, using nanofluids instead of water can augment the performance indices marginally i.e. just around 1%. In addition, it is found that in high temperatures using SiO_2/water nanofluids, which have a lower effective thermal conductivity than that of Cu/water nanofluids, provides higher performance indices.

Keywords: Nanofluids; Solar desalination; Heat exchanger; Freshwater yield

1- Introduction

Nowadays, "Nano" and "Energy" have been two hot keywords, not only in the scientific community but also in our daily life. During recent decades, researchers have attempted to apply nanotechnology to various energy and power systems such as electric generators, fuel cells, batteries, and solar cells [1-5]. Nanotechnology has also been implemented to enhance the heat transfer potential of common liquids like water and oil to ameliorate the efficiency of thermal systems; this can be done through adding solid nanoparticles (particles with a size of 1-100 nm) to the liquids. The mixture of nanoparticles and conventional liquids is named "nanofluid" [6]. Despite some limitations such as relatively high preparation cost and stability issues, extensive attempts have been made to develop the applications of nanofluids in energy systems such as solar energy based devices [7-13], cooling and thermal management of electronic equipment [14,15], grinding and drilling, absorption systems, medicine, heating and cooling of buildings, domestic refrigerators, and so on [16, 17].

In recent years, the problems of global warming and increase of the world population have highlighted the drinking water crisis. Although water covers more than 70% of the earth, most of this is not drinkable. Therefore, providing potable water has always been a major problem for governments and researchers. One of the solutions to overcome the deficiency of freshwater, especially in arid areas, is the usage of solar stills. The main advantage of solar stills is the use of solar energy, a free and clean source, as the driving force for desalination; albeit, on the other hand, their overall efficiency is relatively small. In 2012, Gnanadason et al. [18] investigated experimentally the effect of using carbon nanotubes (CNTs)-based nanofluids on the

performance of a single slope solar still equipped with a vacuum pump. They concluded that adding nanofluids to the basin of solar still can enhance the efficiency up to 50%.

Kabeel et al. [19] experimentally investigated the effects of using a fan as well as adding copper oxide and aluminum oxide based nanofluids into the basin on the productivity of a conventional solar still. For a mass concentration of 0.2% and the use of a fan, it was found that using copper oxide, and aluminum oxide nanofluids increased the productivity by 134% and 125%, respectively. In an economic analysis, they concluded that the use of nanoparticles and the fan lowered the final price of one-liter drinking water compared to conventional solar stills. Kabeel et al. [20] evaluated the effect of using aluminum oxide based nanofluids and a fan with variable speeds and reported a maximum enhancement of 116% for a nanofluid volume concentration of 0.2% under the highest speed of the fan. In another work, Omara et al. [21] experimentally compared the productivity of two solar stills with different configurations. The first was a conventional single slope solar still without any modification while the structure of the second one was modified by corrugated and wick absorbers, an internal reflector, and an external condenser. In addition, copper oxide, and aluminum oxide were added into the basin of the second solar still. The authors concluded that productivity of modified solar still using copper oxide nanoparticles was nearly 285% higher than that of conventional solar still while in the case of aluminum oxide the productivity enhancement was about 255%. Elango et al. [22] prepared four different water-based nanofluids with a concentration of 0.1%, which included aluminum oxide, zinc oxide, iron oxide, and tin oxide for adding to the basin of a single slope solar still with a water depth of 1cm. They found that nanofluids containing iron oxide had no sufficient stability to be used in the tests, so they performed experiments with the other three nanofluids. Their results indicated that the amount of productivity of solar still was directly proportional to the effective thermal conductivity of the nanofluid that was added to the basin. The maximum enhancement in solar still productivity was nearly 30%, which was obtained by aluminum oxide nanoparticles. The productivity improvement values caused by zinc oxide and tin oxide based nanofluids were 19% and 13%, respectively.

In 2016, Sahota and Tiwari [23] theoretically investigated the effect of adding alumina oxide nanoparticles on the productivity of a passive double slope solar still. The analysis was done for three different mass concentrations (i.e., 0.04%, 0.08%, and 0.12%) and two values of water

mass in the basin (35 and 80 kg). They found that the productivity was increased by 12.2% and 8.4% for water masses of 35 and 80 kg, respectively. Later, Sahota and Tiwari [24] modeled a double slope solar still using three different inorganic based nanofluids including alumina oxide, titanium oxide, and copper oxide at a mass concentration of 0.25%. They found that the thermal and exergy efficiencies of the solar still were maximized by using alumina oxide. The thermal and exergy efficiencies alumina-water based solar still were approximately 13% and 9% higher than those of conventional ones, respectively. In another paper, Sharshir et al. [25] experimentally studied the effect of graphite and copper oxide micro-flakes with concentrations between 0.125% and 2% on the productivity of solar stills where the glass cover was chilled by flowing water. The depth of working fluid in the basin was changed from 0.25 to 5 cm, and the mass flow rate of cooling water running on the glass cover varied between 1 and 12 kg/h. The main conclusion of their work was that using graphite particles ameliorated the productivity about 57.6 % while copper oxide particles enhanced the yield by 47.8%.

From the review of the abovementioned articles, it can be concluded that in all of them, nanoparticles were in a direct contact with water inside the solar still basin and there is no any research that investigates both experimentally and theoretically the integration of a solar still to solar collectors through a heat exchanger containing a nanofluid. The motivation behind the present research is based on some reports on the extraordinary enhancement of heat transfer rate caused by nanofluids. Here, two of these reports are mentioned briefly.

Ding et al. [26] experimentally investigated the laminar flow of CNTs/water nanofluids at very low concentrations (0.5%) in a horizontal pipe with a short length (less than 1m). They found that the heat transfer rate was increased by 350%. In another experimental work, Xie et al. [27] studied the heat transfer of MgO based nanofluids in a pipe with constant temperature boundary condition under laminar flow. They reported an enhancement as high as 250% in the heat transfer rate for a nanoparticle volume fraction of 1% at Reynolds number of 1000.

Such an extraordinary potential of nanofluids in heat transfer enhancement encouraged us to study the effects of using nanofluids on the evaporation rate of water inside the basin of a solar still equipped with a heat exchanger. The present study aims at giving a comprehensive analysis of the influence of nanofluids on the productivity as well as the energy and exergy efficiencies of a single slope solar still equipped with a heat exchanger through experiments and mathematical

modeling. The effects of various parameters including nanofluid type, concentration and size of nanoparticles, mass flow rate of working fluid, water depth in the basin, and inlet temperature to heat exchanger have been carried out in this study. In addition, a discussion has been presented for the physical reasons behind the effective parameters on the evaporation rate in the solar still.

2- Experimental Set-up and Procedure

2.1. Experimental Materials

Figure 1 illustrates a schematic diagram of the experimental set-up. The main parts of the set-up include two flat plate solar collectors connected in series, a single slope solar still equipped with a heat exchanger, and a tank for nanofluid supply. After being heated in the solar collectors, the nanofluid enters the heat exchanger installed inside the basin of the solar still to exchange heat with the brackish water and then returns to the nanofluid tank. The basin water evaporates due to the direct solar radiation received as well as heat added by the heat exchanger. The vapor thus created rises from the basin water surface and is condensed on the inner surface of the glass cover. Due to the slope of glass, the condensed water droplets flow towards a channel which collects fresh water. The surface area of the solar still is 0.425 m^2 (length of 85cm and width of 50cm), and total effective surface area of the two flat plate solar collectors is about 4.6 m^2. To have the maximum solar radiation on the solar still during the year, the glass cover slope is adjusted to be equal to the latitude of test location (King Mongkut's University of Technology Thonburi, Bangkok, Thailand), which is approximately 13^o. The solar still body is made of stainless steel while the heat exchanger is fabricated from copper pipes. To minimize heat loss from the solar still body to the environment, the bottom and the side walls of the still were insulated. To measure the temperature at different points of the system (i.e., inlet and outlet of the heat exchanger, inside and outside of the solar still), T-type thermocouples with an accuracy of ±0.1% have been used. Thermocouples are calibrated using Fluke Calibrator.

The performance of a solar still strongly depends on the temperatures of basin water and the inner surface of the glass cover. The reported value for basin water temperature (T_w) is the

average of temperatures given by three thermocouples inserted in different locations of the basin. Additionally, the inner surface temperature of the glass cover is estimated by measurements of the ambient temperature (T_a) and the temperature of the outer surface of the glass ($T_{g,o}$) as:

$$T_{g,in} = \left(T_{g,o} \left(\frac{k_g}{L_g} + h_{t,g,a} \right) - T_a h_{t,g,a} \right) \left(\frac{L_g}{k_g} \right) \quad (1)$$

where L_g and k_g are the thickness and the thermal conductivity of the glass cover, respectively. The parameter $h_{t,g,a}$ is called the total heat transfer coefficient between the glass and the ambient which is a function of wind velocity (V_W) [28]:

$$h_{t,g,o-a} = 5.7 + (3.8 \times V_W) \quad (2)$$

It should be mentioned that the values of wind velocity have been taken from a meteorological center. Solar radiation intensity is measured by Lambrecht pyranometer with an accuracy of ± 5%. To calculate the solar radiation on titled surfaces the method described in APPENDIX A has been used. The values of temperature and solar radiation were recorded with the aid of a data logger (Model NI9213) and LabVIEW software. Water based nanosuspensions (nanofluids) containing silica nanoparticles have been prepared at different volume concentrations of 0.5, 1, and 2% through a two-step approach as follows. For the preparation of a given concentration of nanofluids, a specific amount of silica nanoparticles was added to water gradually while a stirrer was used for a half-hour to mix nanoparticles and water. Next, the mixture was sonicated in an ultrasonic bath for 2-3 hours to break down the agglomeration between particles to increase the nanosuspensions stability. To assess the effect of nanoparticle size on the performance of solar still, nanoparticles with two different sizes including 7 and 40 nm were tested. It should be mentioned that the size of nanoparticles has been verified by the company through TEM images.

2.2. Experimental Procedure

Experiments have been done during sunny days of 2014 and 2015 from 9 AM to 4 PM. The experiments were conducted for different values of volume flow rate of nanofluid (3, 4, and 5 lit/min which are equal to 5×10^{-5}, 6.67×10^{-5}, and 8.33×10^{-5} m^3/s, respectively), nanofluid concentration (0, 0.5, 1 and 2%), nanoparticle size (7 and 40 nm), and water depth of basin (4

and 8 cm). Among various experimental datasets, the results of 24 days have been selected to be reported. Table 1 presents the considered conditions in the selected tests. At the end of each day, the amount of condensed water was measured by a weight scale with an accuracy of 10^{-6} kg.

3- Mathematical modeling

This section deals with mathematical modeling of the solar still which includes the analysis of first and second laws of thermodynamics. For modeling the solar still, it is needed to introduce the measured data of solar radiation, ambient temperature, wind velocity, and the heat exchanger inlet temperature as the inputs of the model. Figure 2 displays the schematic diagram of thermodynamic model considered for the single slope solar still along with top side view. As seen, different heat transfer modes including conduction, convection, radiation, and evaporation are involved in the modeling. It should be mentioned that evaporation from water surface has the dominant effect on heat transfer rate inside the solar still. In the following, the analysis of the thermodynamics laws has been given.

3.1. First law of thermodynamics

The energy equation should be written for the main parts of solar still which are glass cover, water, heat exchanger, and basin liner.

Energy equation for inner surface of glass cover:

By considering the inner surface of glass as control surface and neglecting the heat capacity of glass, the energy equation for this component can be written as [29]:

$$(1-R_g)\alpha_g I_S(t)+(h_{r,w-g,i}+h_{ev,w-g,i}+h_{c,w-g,i})(T_w-T_{g,i})=\frac{k_g}{L_g}(T_{g,i}-T_{g,o}) \quad (3)$$

The above equation states that the summation of solar radiation that reaches the inner surface of the glass and the heat that transfers from the water surface to glass is equal to conduction heat transfer through the inner surface of the glass to the outer surface. In this equation, $I_S(t)$ is the solar radiation intensity on the glass cover, R_g and α_g are reflectivity and absorptivity of glass, respectively. In addition, parameters of $h_{r,w-g,i}$ (radiation heat transfer coefficient), $h_{ev,w-g,i}$

(evaporation heat transfer coefficient), and $h_{c,w-g,i}$ (convection heat transfer coefficient) are defined as follows:

$$h_{r,w-g,i} = \left(\frac{1}{\varepsilon_w} + \frac{1}{\varepsilon_g} - 1 \right)^{-1} \sigma \left[(T_w + 273)^2 + (T_{g,i} + 273)^2 \right] (T_w + T_{g,i} + 546) \quad (4)$$

where σ is the Stefan–Boltzmann constant, also ε_w and ε_g are emissivity coefficients for water and glass, respectively.

In the literature, there are some relations to estimate the evaporation heat transfer coefficient from the water surface to glass cover. One of the most commonly-used equations is Dunkle relation as follows [29-31]:

$$h_{e,w-g,i} = 16.273 \times 10^{-3} \times h_{c,w-g,i} \left[\frac{P_w - P_{g,i}}{T_w - T_{g,i}} \right] \quad (5)$$

where P_w is partial vapor pressure at water surface temperature, and $P_{g,i}$ is partial vapor pressure at glass inner surface temperature. These two later parameters are defined as:

$$P_w = \exp\left[25.317 - \left(\frac{5144}{T_w + 273} \right) \right] \quad (6)$$

$$P_{g,i} = \exp\left[25.317 - \left(\frac{5144}{T_{g,i} + 273} \right) \right] \quad (7)$$

Finally, convection heat transfer coefficient can be estimated by the following equation:

$$h_{c,w-g,i} = 0.884 \left[(T_w - T_{g,i}) + \frac{(P_w - P_{g,i})(T_w + 273.15)}{268.9 \times 10^3 - P_w} \right]^{1/3} \quad (8)$$

Energy equation for outer surface of glass cover:

By considering the outer surface of glass as control surface, the energy equation for this component can be described as follows:

$$\frac{k_g}{L_g} (T_{g,i} - T_{g,o}) = h_{t,g,o-a} (T_{g,o} - T_a) \quad (9)$$

Energy equation for water:

By considering basin water as control volume, and the presence of heat exchanger, the energy equation for basin water becomes:

$$M_w C_w \frac{dT_w}{dt} = A_b \alpha'_w I_S(t) + (A_b - A_{H.E.}) h_w (T_b - T_w) - h_{t,w-g,i} A_b (T_w - T_{g,i}) + Q_u \quad (10)$$

in which

$$h_{t,w-g,i} = (h_{c,w-g,i} + h_{r,w-g,i} + h_{ev,w-g,i}) \quad (11)$$

$$M_w = \rho_w (A_b d_w - V_{H.E.}) \quad (12)$$

$$\alpha'_w = (1-\alpha_g)(1-R_g)(1-R_w)\alpha_w \quad (13)$$

$$Q_u = n\, \dot{m}_{riser,H.E.}\, C_{p,nf} (T_{i,H.E.} - T_{o,H.E.}) \quad (14)$$

where M_w is the mass of basin water, d_w is the depth of water in the basin, A_b is the surface area of basin, $V_{H.E.}$ is the volume of heat exchanger, R_w and α_w are reflectivity and absorptivity coefficients of water, $A_{H.E.}$ is the surface area of heat exchanger, n is the number of heat exchanger risers, Q_u indicates the heat transfer rate between basin water and heat exchanger, ρ_w and C_w are density and heat capacity of basin water, $C_{p,nf}$ is the heat capacity of nanofluid flowing in the heat exchanger, and h_w is the convection heat transfer coefficient between basin liner and water which is obtained as [32]:

$$h_w = \frac{\overline{Nu}_L k_w}{L_c} \quad (15)$$

where:

$$\begin{cases} \overline{Nu}_L = 0.54 Ra_L^{1/4} & (10^4 \le Ra_L \le 10^7) \\ \overline{Nu}_L = 0.15 Ra_L^{1/3} & (10^7 \le Ra_L \le 10^{11}) \end{cases} \quad (16)$$

$$Ra_L = \frac{g\beta_w (T_b - T_w)(L_c)^3}{\alpha_w \upsilon_w} \quad (17)$$

In the above, α_w, υ_w, and β_w are the thermal diffusivity, kinematic viscosity, and thermal expansion coefficient of basin water, respectively. Also, L_c represents the ratio of surface area to perimeter of the basin.

Energy equation for basin liner:

The net energy absorbed by the basin liner is equal to the summation of heat transfer from basin liner to basin water and heat loss from bottom to the environment. Therefore, the energy equation for basin liner can be written as:

$$\alpha'_b I_S(t) = h_w(T_b - T_w) + h_b(T_b - T_a) \tag{18}$$

where:

$$\alpha'_b = \alpha_b(1-\alpha_g)(1-R_g)(1-R_w)(1-\alpha_w) \tag{19}$$

$$h_b = \left[\frac{L_{ins}}{k_{ins}} + \frac{1}{h_{t,b-a}}\right]^{-1} \quad ; \quad h_{t,b-a} = 5.7 + (3.8 \times V_W) \tag{20}$$

In the above, h_b is the heat transfer coefficient from the basin liner to the environment, also, L_{ins} and k_{ins} are thickness and thermal conductivity of insulator which covers the bottom of solar still.

Energy equation for heat exchanger:

The energy equation for heat exchanger can be written as:

$$\frac{dT_f}{dx} + AT_f(x) = B \tag{21}$$

in which A and B are defined as follows:

$$A = \frac{\pi d_{riser,H.E.} h_{nf,H.E.}}{\dot{m}_{riser,H.E.} C_{p,nf}} \tag{22}$$

$$B = \frac{\pi d_{riser,H.E.}\left[\frac{\alpha'_{H.E.}}{2} I_S(t) + h_{nf,H.E.} T_w\right]}{\dot{m}_{riser,H.E.} C_{p,nf}} \tag{23}$$

in the above, $h_{nf,H.E.}$ is the convection heat transfer coefficient of nanofluid inside the heat exchanger risers. The value of $\alpha'_{H.E.}$ is assumed to be 0.7.

To solve Eq. (21), it is needed to know the inlet temperature of nanofluid to the heat exchanger which is imported from experimental data to the model.

So, by having $T_f(x=0) = T_{i,H.E.} = \text{known}$, the outlet temperature of nanofluid is obtained by solving Eq.(26):

$$T_{o,H.E.} = (T_{i,H.E.} - \frac{B}{A})e^{-AL} + \frac{B}{A} \tag{24}$$

The parameter of $h_{nf,H.E.}$ determines the role of nanofluids on the evaporation rate. It can be estimated through the definition of Nusselt number as follows:

$$h_{nf,H.E.} = \frac{Nu_{nf,H.E.} k_{nf}}{d_{riser,H.E.}} \tag{25}$$

By considering the range of mass flow rate of nanofluids in the experiments as well as the size of rises it is found that the flow in heat exchanger risers is laminar. In addition, since the length of heat exchanger risers is relatively short (about 70 cm) so the flow is hydrodynamically and thermally developing [32]. One of the well-known equations that can be used to estimate the Nusselt number in laminar regime, where the flow is hydrodynamically and thermally developing, is the correlation presented by Sieder and Tate [32] as:

$$Nu_{nf,H.E.} = 1.86\left(Re_{nf,H.E.} Pr_{nf,H.E.} \frac{d_{riser,H.E.}}{L_{riser,H.E.}}\right)^{1/3}\left(\frac{\mu_{nf}}{\mu_w}\right)^{0.14} \tag{26}$$

The above relation can be used under the following conditions:

$$\begin{cases} T_S = \text{constant}\,;\, 0.48 \le Pr_{nf} \le 16700 \\ 0.0044 < \left(\dfrac{\mu_{nf}}{\mu_w}\right) < 9.75 \\ \left(Re_{nf,H.E.}\, Pr_{nf,H.E.}\, \dfrac{d_{riser,H.E.}}{L_{riser,H.E.}}\right)^{1/3} \left(\dfrac{\mu_{nf}}{\mu_w}\right)^{0.14} \ge 2 \\ \text{in which}: Re_{nf,H.E.} = \dfrac{4\dot{m}_{riser,H.E.}}{\pi\, d_{riser,H.E.}\mu_{nf}}, Pr_{nf,H.E.} = \dfrac{\mu_{nf}\, C_{P,nf}}{k_{nf}} \end{cases} \quad (27)$$

As indicated above, Sieder and Tate relation is valid for a wide range of Prandtl numbers; so it is useful for nanofluids at different concentrations as well. The results of some studies on nanofluids clearly show that Sieder and Tate correlation can predict the Nusselt number of nanofluid flows with high accuracy, especially at low concentrations of nanofluids (i.e., lower than 2%). To estimate the thermal conductivity and viscosity of nanofluids, the correlations given by Sharma et al. [33] have been used.

The hourly productivity of solar still (m_{ew}) in terms of (kg/m^2h) is ascertained as follows:

$$m_{ew} = \frac{h_{e,w-g,i} \times (T_w - T_{g,i})}{h_{fg}} \times 3600 \quad (28)$$

in which h_{fg} is the latent heat of vaporization (kJ/kg). It reads as [34]:

$$h_{fg} = 3161.5 - 2.40741 \times (T_w + 273.15) \quad (29)$$

In this work, the duration of experiments was 7 hours (9 AM- 4 PM), so the total productivity of solar still is obtained by:

$$M_{ew} = \sum_{i=1}^{7} m_{ew} \quad (30)$$

For heating of nanofluids, two flat plate solar collectors have been used. Therefore, to calculate the efficiency of solar still in a specific period of Δt, the solar radiation on flat plate solar collectors should be taken into account as well. The solar still efficiency is described as [29]:

$$\eta_{th,ss} = \frac{\sum m_{ew} \times h_{fg}}{\sum I_S(t) \times A_b \times \Delta t + \sum I_{S.C.}(t) \times A_C \times \Delta t} \quad (31)$$

where A_C is the surface area of solar collector, and $I_{S.C.}(t)$ is the solar radiation on the collector surface.

The system of equations presented in this section has been solved by iterative approach.

3.2. Second law of thermodynamics

The performance of a thermal system can be optimized through exergy analysis. To calculate the exergy efficiency of the solar still, besides the amount of the solar radiation on solar still and the two collectors, it is needed to know the temperatures of ambient, basin water, and the inner surface of glass. Exergy efficiency of the solar still is defined as [29, 35]:

$$\eta_{EX,ss} = \frac{\dot{E}x_{evap}}{\dot{E}x_{input}} \quad (32)$$

where $\dot{E}x_{evap}$ is the output exergy of solar still estimated by:

$$\dot{E}x_{evap} = \dot{E}x_{output} = h_{e,w-g,i} \times A_b \times (T_w - T_{g,i}) \times \left(1 - \frac{T_a + 273}{T_w + 273}\right) \quad (33)$$

and $\dot{E}x_{input}$ is the input exergy to solar still, it can be demonstrated as:

$$\dot{E}x_{input} = \dot{E}x_{sun}(\text{solar still}) + \dot{E}x_{sun}(\text{solar collector}) \quad (34)$$

$$\dot{E}x_{sun}(\text{solar still}) = A_b \times I_S(t) \times \left[1 - \frac{4}{3} \times \left(\frac{T_a + 273}{T_{sun}}\right) + \frac{1}{3} \times \left(\frac{T_a + 273}{T_{sun}}\right)^4\right] \quad (35)$$

$$\dot{E}x_{sun}(\text{solar collector}) = A_{S.C.} \times I_{S.C.}(t) \times \left[1 - \frac{4}{3} \times \left(\frac{T_a + 273}{T_{sun}}\right) + \frac{1}{3} \times \left(\frac{T_a + 273}{T_{sun}}\right)^4\right] \quad (36)$$

where T_{sun} indicates the surface temperature of the sun and assumed to be 6000 K. It should be mentioned due to low consumption of pump, its corresponding exergy has been neglected.

4- Results and discussion

The results have been presented in two parts. In the first part experimental results, and in the second part the results of numerical simulation are rendered.

4.1. Experimental results

To validate the present experimental results, some comparisons have been made with available correlations in the literature. Rahbar and Esfahani [36] presented a correlation to estimate the productivity of single slope solar stills. The correlation was as a function of glass cover and water temperatures. By considering 24 selected days; the comparison between present experimental results and the correlation given in [36] showed that the average deviation does not exceed 6%. Two important environmental parameters that affect the efficiency of solar still are the radiation and ambient temperature. The productivity of solar still will increase with a higher solar radiation. On the other hand, at a given value of solar radiation, the productivity increases with a decrease in ambient temperature. The reduction of ambient temperature leads to the temperature reduction of glass cover as the condenser. Figure 3 presents the total solar radiation (from 9 AM to 4 PM) on the solar still and two solar collectors for the selected days that are indicated in Table 1. As seen, for the first six days, the amount of radiation on the surfaces of two collectors, which have been installed with slopes of 35^{o} and 37^{o} on horizontal, are nearly equal, and higher than that of the solar still with glass cover having a slope of 13^{o}. For the remaining days (7 to 24), the amount of solar radiation on solar still is higher than those of solar collectors. It should be noted that the data of the first six days have been collected in December (winter) and the datasets of the other days belong to the summer season. In summer, the amount of solar radiation on surfaces with a lower slope is higher because the sun shines perpendicular to the earth surface, however in winter the surfaces with smaller inclination receive lower radiation.

Figure 4 shows the average ambient temperature during the selected days. As seen, the temperature difference between the coldest day (5^{th} day) and warmest day (23^{rd} day) is more than 10 ^{o}C. As mentioned above, the data of the first six days were collected during winter.

Figure 5 (a-c) exhibits the values of performance indices of solar still including yield, thermal efficiency, and exergy efficiency during different days. As observed, the trends of the three indices are different. By considering Fig. 5 (a) and Fig. 3 (total solar radiation), it unveils that the quantity of yield has been a strong function of solar radiation and the effects of working fluid

type, mass flow rate, and water depth in the basin have been negligible. For example, solar still productivity was maximized for the 8th day because in this day the amount of solar radiation on the solar still was highest, and in addition the amount of radiation on the two collectors was relatively high. The minimum productivity was obtained for the 24th day; even lower than winter days (days of 1to 6). It should be noted that although for the 24th day the solar radiation on solar still is higher than those of winter days, the value of solar radiation on solar collectors is lower for the 24th day in comparison with winter days. Therefore, the working fluid absorbs less heat in solar collectors for the 24th day that affects the yield. Another reason behind the lower productivity for the 24th day compared to winter days may be the higher ambient temperature in this day, since it leads to the increase of condenser temperature, and, consequently, lowers the productivity. It should be mentioned that the working fluid for the 8th day was nanofluid with a volume fraction of 0.5% whereas for the 24th day it was nanofluid with a concentration of 2%.

Figure 5 (b) shows the variations of thermal efficiency in different days. As shown, the efficiency of solar still was highest for the 9th day while the productivity for the 9th day was less than that of the 8th day. The energy efficiency of solar still has an inverse relation with the received radiation by solar still and solar collectors. Since the radiation received by the system for the 8th day was higher than that of the 9th day, therefore, the corresponding efficiency for the 8th day becomes less. The maximum experimental thermal efficiency was 3.28% while the minimum value was 2.19%. In this work, the existence of solar collectors could improve the yield of solar still. However, it reduces the thermal efficiency levels due to large surface area of the absorbers. Figure 5 (c) shows the exergy efficiency during different days. As illustrated, exergy efficiency for the 12th day was maximum, and its value was even more than those of 8th and 9th days that had the maximum productivity and thermal efficiency, respectively. Equations (32-36) elucidate that ambient temperature plays a significant role in the exergy efficiency magnitude. With an increase in the ambient temperature, the output exergy decreases while the input exergy increases and this consequently leads to the reduction of exergy efficiency. Fig. 4 reveals that the average ambient temperature for the 12th day is about 2 ^{o}C lower than those of 8th and 9th days which is the reason behind the higher exergy efficiency for the 12th day. Figure 5(a-c) indicates that the most vital parameters affecting the solar still performance are solar radiation and ambient temperature, and not the nanofluid concentration and/or mass flow rate of the working fluid.

4.2. Mathematical model verification

The experimental results indicated that the performance indices of solar still strongly depend on solar radiation and ambient temperature. Since the experiments have been done in different days, and, consequently, different weather conditions, the effect of nanofluid on the evaporation rate in the solar still cannot be specified precisely. Therefore, it is needed to accommodate a mathematical model to determine the exact effects of nanofluid on solar still performance. It should be noted, however, that the experimental study is vital to validate the results of the mathematical modeling.

First, let us define the following parameter:

$$\text{R.D.}(\%) = \left| \frac{\text{Experiment} - \text{Theory}}{\text{Theory}} \right| \times 100 \tag{37}$$

where R.D. is the ratio difference between experimental and theoretical results.

Figure 6(a-c) presents comparisons between experimental data and theoretical results for yield, thermal efficiency, and exergy efficiency of the solar still. As shown in the figure, there is a reasonable agreement between experimental and simulation results. In the case of solar still yield (Fig. 6(a)), the minimum R.D. is 2.3% while the maximum R.D. reaches 14.3%. Moreover, the average value of R.D. (considering 24 days) is about 9%. In the case of thermal and exergy efficiencies, it is found that the average value of R.D. does not exceed 11%. The amounts of R.D. for the 12^{th} day have been highlighted in Fig. 6 since the weather conditions on this day will be used in the next sections. As can be seen from Fig. 6, the values of R.D. for yield and thermal efficiency are less than 3% for the 12^{th} day, and those for exergy efficiency are less than 6%. The reason behind selecting the metrological data of 12^{th} day is as follows: The uncertainty in the determination of solar radiation can be a source of difference between experimental and modeling results. We selected the data of 12^{th} day because the difference between experimental and modeling results are low. One of the reasons behind this small difference may be the low errors in solar radiation determination. One may ask why the weather conditions related to the 3rd day that has lower R.D. are not used. We preferred to use the data on the 12^{th} day since the working fluid in this day was nanofluid while on the 3rd day the working fluid was water. Figure 7 (a-c) shows comparisons between the experimental and the simulation results for temperatures

of basin water, outlet heat exchanger, and glass cover on the 12th day. As can be observed from Fig. 7 (a, b), the average values of R.D. for the temperatures of basin water and the outlet heat exchanger are less than 1%. The small value of the average R.D. for the basin water temperature reveals that assumption of a uniform distribution for the temperature in the basin water is acceptable since the water depth in the solar still is relatively low. However, as shown in Fig. 7 (c), the average R.D. is relatively high (about 6%) in the case of the glass cover temperature. The values of R.D. for the glass cover temperature are greater between 1 and 3 PM. The main possible reasons behind the difference between experimental data and modeling results (considering Figs. 6 and 7) are discussed in the following.

1) Error in estimating the amount of radiation: Among the environmental factors such as radiation, wind speed, and ambient temperature, solar radiation has the greatest impact on the performance of solar still. In this study, the solar radiation on horizontal surfaces has been measured, and a semi-empirical relation has been used to estimate the solar radiation on tilted surfaces which can involve some errors in the determination of radiation. On the other hand, the pyranometer that is used in the experiments measures the solar radiation with an uncertainty of ±5%. That also contributes to the errors in estimating the radiation.

2) The effect of specific heat capacity of the glass cover, basin liner, and heat exchanger: In most of the studies on solar stills, only the specific heat capacity of water has been included in the modeling. Considering the heat capacity of the glass cover, basin liner and heat exchanger can increase the accuracy of the model somewhat.

3) Effect of heat losses: The effect of heat losses from side surfaces has been neglected in the model. Taking these losses into account may help to improve the accuracy.

4) Error in estimating the temperature of the glass: As mentioned above, the model can predict the temperature of the water in the basin with good accuracy, but the amount of error in estimating the glass temperature is higher than that of the basin water. This may be due to the errors in the estimation of convection and radiation heat transfer coefficients between the water surface and the glass as well as that between the outer surface of the glass and the environment. Another source of error may be attributed to the uncertainty in the physical and optical properties of the glass material.

5) Error in the estimation of Nusselt number for heat exchanger: Determining the exact value of Nusselt number for nanofluid flow in the heat exchanger is not easy. Therefore, the uncertainty in the value of the Nusselt number can be a source of error in the modeling. In the next section, a comprehensive discussion on the role of Nusselt number in the modeling of solar still is presented.

In conclusion, despite the error sources mentioned above, the presented model gives reasonable estimations of solar still performance.

4.2.1. Nusselt number effect

In order to show how much significant the Nusselt number value is in the estimation of solar still performance, two different cases have been considered. In the first case, similar to some reports in the literature, it is assumed that the flow in risers is fully developed, therefore, the value of the Nusselt number is 3.66 (note that the boundary condition for risers is taken as constant temperature). In the second case, the Nusselt number has been estimated based on the real condition, i.e., developing flow. In this case, the value of Nusselt number for the 12^{th} day becomes 6.51 which is about 77% higher than that of fully developed flow assumption. In a given nanofluid concentration, a higher Nusselt number leads to a higher heat transfer coefficient in the solar still and consequently evaporation rate is augmented. The results of comparison between these two cases have been presented in Fig. 8. As can be seen from the figure, the deviation of simulation results from the experimental ones for yield and thermal efficiency is approximately 3 % when considering developing flow. On the other hand, when the flow is assumed to be fully developed the deviation reaches about 6% (i.e., nearly 3% increase in deviation). Moreover, in the case of exergy efficiency, the fully developed assumption leads to increase the deviation from about 6% to more than 10%. It should be noted that experimental studies on nanofluids reveal that by increasing the mass flow rate (or Reynolds number), and concentration of nanofluid, the accuracy of Sieder and Tate relation decreases since it underestimates the value of Nusselt number (for example see Ref.[37]). The reasons behind the inaccuracy of Sieder and Tate relation in the estimation of Nusselt number are discussed in the following sections.

Brownian motion effect

There are some reports in the literature showing that the Brownian motion is a significant parameter in the thermal conductivity enhancement of nanofluids, and, hence the heat transfer enhancement (for example see Ref. [38]). Brownian motion increases heat conduction in the media through the increase of collisions between molecules. Although the effect of Brownian motion is included in the experimental based correlation on thermal conductivity given by Sharma et al. [33], it should be noted that the nanofluid thermal conductivity has been measured in a stationary condition. The intensity of Brownian motion increases with moving nanoparticles in heat exchanger risers, which is subjected to forced convection. Thus, it is expected that the heat diffusion is enhanced. The Brownian motion is not considered in Sieder and Tate relation.

Nanoparticles migration from pipe wall

In forced convection flow in risers, the shear rate on the riser wall is the highest while it is the lowest at the centerline of the riser. On the other hand, it is established that nanoparticles tend to move from a region with a higher shear rate to a region with a lower shear rate and this leads to a decrease of viscosity in the vicinity of riser wall [39]. As the viscosity decreases, the boundary layer thickness reduces, and, hence, the heat transfer coefficient ameliorates. Since Sieder and Tate relation is developed for common liquids and not for mixtures of solid and liquids, the migration of particles is not considered in developing it.

Increasing the wettability by nanofluid

Investigations have shown that the wettability of nanofluids is higher than that for the common liquids such as water [39]. In other words, from the microscopic viewpoint, the contact angle of a nanofluid droplet with wall surface is smaller than that of a water droplet; this leads to increase the heat transfer rate.

Effect of surface roughness

In the correlation presented by Sieder and Tate, the effect of surface roughness of pipe is not considered. Although the flow regime in this study is laminar, however, Gloss and Herwig [40] showed that the roughness effect is not negligible in laminar flow. In addition, in 1936, Wenzel indicated that the wettability of liquid increases with increasing the surface roughness [41]. As mentioned before, a higher wettability provides a higher heat transfer coefficient. It can be

concluded that there is a need to develop a new correlation involving the effect of surface roughness of tube.

Aggregation of nanoparticles

In some studies, the aggregation of nanoparticles is shown to decrease the heat conduction in nanofluids (for example see Ref. [42]). However, in some other studies, the aggregation of nanoparticles is listed as a factor for the heat conduction enhancement [43, 44]. In 2017, Cai et al. [44] highlighted the positive effect of nanoparticles' aggregation in heat conduction augmentation through fractal analysis.

Diffusiophoresis

Concentration gradient in a system is responsible for the phenomenon of diffusiophoresis. In this phenomenon, nanoparticles tend to move from a region with higher concentration to a region with a lower concentration to attain equilibrium in the system. As noted, nanoparticles tend to migrate towards the centerline of the pipe due to the high shear rate at the wall surface, but on the other hand, diffusiophoresis prevents this migration to make a balance in the concentration. The interaction between diffusiophoresis mechanism and migration of nanoparticles caused by different shear rates in the riser can increase the turbulence in the boundary layer that leads to the heat transfer enhancement. Figure 9 graphically summarizes the microscopic and nanoscopic phenomena occurring inside the heat exchanger that affect the evaporation rate in the solar still.

It should be noted that effects of nanoparticles on the boundary layer growth are very complex and more investigations are needed to identify these effects on the heat transfer enhancement of nanofluids.

4. 3. Modeling results

After the model validation, first the role of heat exchanger on the solar still performance has been investigated. Next, the effect of nanofluids on the magnitude of heat transfer enhancement in the heat exchanger is discussed. Finally, the effects of different parameters such as nanofluid concentration, nanoparticle size and type, mass flow rate of nanofluid, and water depth in the

basin on the evaporation rate in the solar still are investigated under identical weather conditions where the nanofluid enters the heat exchanger at different constant temperatures in the range of 35 -70 ^{o}C. Here, it does not matter how the nanofluid is heated; the main point is that the nanofluid enters the heat exchanger at a constant temperature during the solar still operating period. Therefore, the energy consumed by the solar collector or any other heater is not considered in the calculation of system efficiency. It should be noted that the weather conditions of the 12th day including solar radiation, ambient temperature, and wind velocity have been introduced as inputs in the mathematical model. In the present analysis, the SiO_2/water nanofluids considered to be the base case, and comparisons have been done with the case of the Cu/water nanofluid.

4.3.1. On the role of heat exchanger

The first question that comes to mind that how much is the effect of the heat exchanger on the evaporation rate enhancement in the solar still? In other words, is it helpful to use the heat exchanger in the solar still? If yes, for which range of inlet temperatures, the heat exchanger can improve the evaporation rate? In this respect, Fig. 10 is plotted to answer the question. Figure 10 compares the solar still performance indices for the inlet temperatures of 50, 60, and 70 ^{o}C with performance indices of a solar still without heat exchanger (called classic solar still or CSS). As shown, when the inlet temperature of working fluid to the heat exchanger is 70 ^{o}C, the amounts of yield, energy efficiency, and exergy efficiency are more than two times higher than those of the solar still without the heat exchanger. In addition, it is observed that when the inlet temperature is 50 ^{o}C, the yield is about 81% less than the solar still without heat exchanger; this implies that using heat exchanger when the inlet temperature is $\leq$ 50 ^{o}C is not useful and leads to the reduction of performance indices. At the beginning of system operation when the working fluid enters the heat exchanger at a low constant temperature (e.g. 50 ^{o}C) it may increase the temperature of basin water and consequently it may lead to the increase of evaporation rate inside the solar still, since the water temperature is not still high (about 35 ^{o}C). However, when time passes and solar radiation intensity increases, the temperature of basin water reaches a value higher than that of the heat exchanger inlet temperature; therefore, the working fluid acts as a cooler and keep the temperature of basin water around 50 ^{o}C. In the same time, the temperature of glass cover raises due to solar radiation. Hence, the temperature difference between glass

cover and basin water reduces considerably, which acts as a deterrent to water evaporation and freshwater production. However, when the inlet temperature is high, for example 70 ^{o}C, the effect of heat exchanger on the evaporation rate is remarkable, especially at the beginning of system operation. At the beginning of system operation, the solar radiation is not so high, so the glass cover has a low temperature; on the other hand, in a short time, the temperature of basin water reaches the heat exchanger inlet temperature (around 70 ^{o}C). The high difference between water basin temperature and glass cover accelerates the evaporation in the solar still. At noon, when the solar radiation increases, although the temperature difference between evaporation and condensation surfaces decreases; but the temperature difference is high enough to act as a driving force for the immigration of vapor drops towards the glass cover. It should be noted that convection and radiation heat transfer between outer side of glass cover and the environment (with temperatures around 30-35^{o}C) decreases the outer surface temperature of glass cover. Consequently, the inner surface temperature of glass cover reduces through heat conduction which prevents the inner surface to reach high temperatures as much as the basin water temperature i.e. 70 ^{o}C.

4.3.2. On the heat transfer enhancement by nanofluids

In the previous section, it was proved that using of a heat exchanger (depends on the inlet temperature value) could be a suitable solution for remarkable enhancement of solar still productivity. In the next step, we focus on the effect of using nanofluids instead of water in the heat exchanger on the heat transfer rate enhancement. Figure 11 illustrates the variations of convection heat transfer coefficient ($h_{nf,H.E.}$), defined in Eq. (25), with concentration and inlet temperature for SiO_2/water nanofluid at d_w = 4 cm and $\dot{m}$ = 0.04 kg/s. It is observed that the heat transfer coefficient enhances with an increase in the volume fraction and inlet temperature. The higher heat transfer coefficient of nanofluids compared to water can be attributed to their greater effective thermal conductivity. As mentioned, Brownian motion of nanoparticles is one of reasons behind the thermal conductivity enhancement of nanofluids that has been included in the experimental-based correlations presented for thermal conductivity. With increasing the inlet temperature from 50 to 70 ^{o}C the kinetic energy of liquid's molecules increases which leads to the enhancement of effective thermal conductivity, and, consequently, the heat transfer coefficient augments. In other words, by replacing nanofluids instead of water as the working fluid the boundary layer thickness in the risers of heat

exchanger decreases, and, hence, the total heat transfer rate from heat exchanger to the basin water increases.

At 50 ^{o}C, heat transfer coefficient of nanofluid with a volume fraction of 4% is about 12.2% higher than that of water while at 70 ^{o}C this amount reaches 15.4%. These statistics prove that the amount of heat transfer enhancement, which is obtained by replacing nanofluids (with a volume fraction of 4%) instead of water, is not ignorable, especially for higher inlet temperatures.

4.3.3. Nanofluid effect on solar still performance

Nanofluid effect on the solar still performance is investigated in three separate parts. First, the effect of nanofluid concentration, and later the effects of nanoparticle type and size are studied.

4.3.3.1. Effect of nanofluid concentration

From the two previous parts, first, it was concluded that using the heat exchanger where the inlet temperature is 70 ^{o}C can enhance the solar still productivity more than 2 times. Next, it was shown that heat transfer coefficient can be augmented 15.4% by replacing nanofluid with a concentration of 4% instead of water in the heat exchanger. Therefore, one may expect to observe favorite effects of nanofluids on the solar still performance since their effect on heat transfer enhancement is not a negligible value. Figures 12-14 are plotted to show the effect of using SiO_2/water nanofluid with a volume fraction of 4% on the solar still performance for three different inlet temperatures of 50, 60, and 70 ^{o}C. The results are presented for mass flow rates between 0.04 and 0.12 kg/s and water depths between 4 and 8 cm. The results indicate that at a volume fraction of 4% and inlet temperature of 70 ^{o}C, despite the increase of convection heat transfer coefficient by 15.4%, exergy efficiency increases approximately 1% while yield and thermal efficiency increase just 0.66%. It is observed that with decreasing the inlet temperature from 70 to 50 ^{o}C, the enhancement rate of solar still performance indices (achieved by using nanofluid instead of water) increases insignificantly. Other observations from Figs. 12-14 are summarized as follows:

- At a given inlet temperature and a specific working fluid, the trend of changes in all of the solar still performance indices is the same. For example, when the productivity increases

with increasing the mass flow rate as well as with the water depth increment, the energy and exergy efficiencies follow the same trend.

- Yield, energy efficiency, and exergy efficiency enhance with raising the inlet temperature of the heat exchanger. As the inlet temperature is increased the difference between temperatures of basin water and glass cover increases, and, consequently the evaporation rate increases.
- With increasing the inlet temperature of the heat exchanger from 50 to 60 ^{o}C, the exergy efficiency increases more than three times (maximum enhancement) while the energy efficiency enhances more than two times (minimum enhancement).
- With increasing the inlet temperature of the heat exchanger from 50 to 70 ^{o}C, the exergy efficiency increases more than seven times (maximum enhancement) while the energy efficiency enhances more than three times (minimum enhancement).
- For inlet temperatures of 60 and 70 ^{o}C, by increasing the mass flow rate, the performance indices enhance regardless of nanofluid concentration and water depth. However, for an inlet temperature of 50 ^{o}C and water depths of 6 and 8 cm performance indices have an ascending trend with mass flow rate. However, at a water depth of 4 cm, there is a mass flow rate in which the performance indices are minimized. The minimum mass flow rate is 0.06 kg/s for water and 0.08 kg/s for nanofluid with the volume concentration of 4%.
- There is a non-linear relationship between performance indices and mass flow rate while there is a linear relation between the performance indices and water depth (See Figs. S1-S3).
- Evaporation rate decreases with an increase in water depth; this occurs because the amount of heat storage capacity in water which corresponds to the product of water mass and the specific heat capacity increases with an increase in water depth, which leads to a reduction in the evaporation rate.

From the results in this section it can be concluded that nanofluid concentration has no significant effect on the improvement of solar still performance. The effect of nanofluid concentration on the performance improvement diminishes with increasing the inlet temperature.

4.3.3.2 Effects of nanoparticles type

Figure 15 shows the effects of nanoparticle type on the yield of solar still at different concentrations for three inlet temperatures of 50, 60, and 70 ^{o}C, two water depths of 4 and 8 cm, and two mass flow rates of 0.04 and 0.12 kg/s. Two different types of nanofluids have been

considered, i.e. SiO_2/water and Cu/water. The size of nanoparticles is 7nm, and the maximum concentration is 4%. It should be noted that the thermal conductivity of Cu nanoparticles is about 400 W/mK that is much higher than that of SiO_2 nanoparticles (1.4 W/mK). In the first glance, someone may think that Cu nanoparticles with a higher thermal conductivity are more effective on the evaporation rate in the solar still, but the results show that this is not always true. The related figures on the effects of nanoparticle type on the thermal and exergy efficiencies are presented in the supplementary files (See Figs. S4 and S5). The following can be found from Figs. 15, S4 and S5:

- At any value of mass flow rate, water depth, and inlet temperature, the performance indices always improve with increases in the SiO_2/water concentration. It implies that the values of performance indices are maximized at the maximum volume fraction that is equal to 4%. However, in the case of Cu/water nanofluids, the ascending trend of performance indices with concentration is seen just at a temperature of 50 ^{o}C. At higher temperatures, i.e., 60 and 70 ^{o}C, it is found that the performance indices are maximized at a volume concentration of 1%.
- For volume fractions of 1% and less, the values of performance indices for Cu/water nanofluid are higher than that of SiO_2/water nanofluid. However, for volume fractions higher than 1% and temperatures of 60 and 70 ^{o}C, it is found that using SiO_2/water nanofluid instead of Cu/water nanofluid leads to increases in the evaporation rate; because under these conditions the amount of convection heat transfer coefficient associated with the SiO_2/water nanofluid flow is higher than that of Cu/water. As known, the Nusselt number is a function of Reynolds and Prandtl numbers. At a given value of volume fraction and mass flow rate, the value of Reynolds number is the same for both nanofluids of Cu/water and SiO_2/water since the Reynolds number depends only on mass flow rate and viscosity. The viscosity of nanofluid is a function of nanoparticle diameter and volume fraction as well as suspension temperature, and it is independent of the type of nanoparticles. Therefore, by assuming identical values of nanoparticle size, suspension temperature, nanoparticle volume fraction, and mass flow rate, the Reynolds number will be the same for both nanofluids. Therefore, the Nusselt number becomes a function of only Prandtl number. From the physical viewpoint, Prandtl number is the ratio of

momentum diffusion to heat diffusion ($\Pr = \frac{\mu C_p}{k}$). For copper (Cu) nanoparticles, the thermal conductivity is much higher than that of silica (SiO_2) nanoparticles. On the other hand, specific heat capacities of copper and silica nanoparticles are, respectively, 385 J/kg K and 745 J/kg K. Therefore, Prandtl number and consequently Nusselt number for copper nanoparticles is smaller in the case of Cu nanoparticles. Moreover, heat transfer coefficient is defined as $h = \frac{Nu \times k}{d}$; based on this definition Nusselt number and thermal conductivity play the key roles in the determination of heat transfer coefficient. Although heat transfer coefficient of copper nanoparticles is higher, but the lower value of Nusselt number for copper particles leads to higher heat transfer coefficient for SiO_2/water nanofluids. For instance, at a volume fraction of 4% when the inlet temperature is 70 ^oC, Prandtl and Nusselt numbers for Cu/water nanofluid are 2.26 and 4.43, respectively, while for SiO_2/water nanofluid the values of Prandtl and Nusselt numbers are 3.04 and 4.89, respectively. This reveals that Nusselt number for SiO_2/water is about 10.4% higher than that of Cu/water. On the other hand, although the thermal conductivity of Cu/water nanofluids is approximately 8.9% greater than that of SiO_2/water nanofluids, however, in sum, heat transfer coefficient for SiO_2/water nanofluid (432.6 W/m^2K) becomes higher than that of Cu/water nanofluid (427.33 W/m^2K). The higher heat transfer coefficient for the case of silica-based nanofluids provides higher evaporation rate in the solar still as compared with copper-based nanofluids.

- It is found that although using nanofluids instead of water in the above-mentioned range of inlet temperature (between 50 and 70 ^oC) can enhance the evaporation rate in the solar still, the amount of enhancement is insignificant. The maximum enhancement in performance indices is observed for an inlet temperature of 50 ^oC, and by increasing in the inlet temperature the rate of enhancement decreases. For example, at inlet temperature of 50 ^oC, water depth of 4 cm, and mass flow rate of 0.04 kg/s where Cu/water is the working fluid, the increase of nanofluid concentration from 0 to 4% leads to about 2.5% enhancement in exergy efficiency while the yield and thermal efficiency increase just about 1.5%.

From the above discussions, it is concluded that using nanofluids instead of water at the temperature range of 50 to 70 ^{o}C does not have a significant influence on the evaporation rate. Furthermore, it is seen that by increasing the inlet temperature, the usefulness of nanofluids decreases so that at a high inlet temperature of 70 ^{o}C, using nanofluid with a relatively high volume concentration of 4% instead of water yields less than 1% improvements in the performance indices.

Subsequently, the effects of nanofluids on the performance indices of solar still where the inlet temperature is less than 50 ^{o}C is investigated.

Figures 16-18 display the performance indices of solar still for the inlet temperature range of 35 to 45 ^{o}C, and the two nanofluids, i.e., Cu/water and SiO_2/water. The results show that at an inlet temperature of 39 ^{o}C, mass flow rate of 0.04 kg/s and water depth of 4 cm, using Cu/water nanofluid instead of water can enhance the yield, thermal efficiency, and exergy efficiency of the solar still by 9.86, 9.91, and 11.8 %., respectively. It should be noted however that the amount of yield for an inlet temperature of 39 ^{o}C is just 0.1 kg/m^{2}day that is negligible. In addition, it is observed that using nanofluids instead of water is more effective at a lower mass flow rate.

The reason behind the significant enhancement in performance indices of solar still at low inlet temperatures (e.g. 39 ^{o}C) can be attributed to the temperature difference between the glass cover and basin water. During the day time, by increasing solar radiation, the temperatures of basin water as well as the glass gradually increase. Since the inlet temperatures are relatively low, the temperature difference between glass and basin water also becomes small so that the effect of increasing of the heat transfer coefficient on the evaporation rate enhancement becomes more sensible. On the other hand, the heat transfer coefficient of nanofluid is higher than that of water; hence, nanofluids present a considerable improvement in evaporation rate. It should be noted that at high inlet temperatures (e.g. 70 ^{o}C), the temperature difference between glass and basin water is relatively high so that the higher heat transfer coefficient of nanofluid compared to water has no ~~a~~ significant effect on the evaporation rate inside the solar still. From Figs. 16-18, it can be concluded that the remarkable enhancement in performance indices of solar still produced by the use of Cu/water nanofluid at an inlet temperature of 39 ^{o}C is not worthwhile from the practical viewpoint since it leads to a considerable decrease of solar still yield.

4.3.3.3. Effects of nanoparticles size

Finally, the effect of nanoparticle size on the performance of solar still has been investigated. The results of this investigation for an inlet temperature of 70 ^{o}C, water depth of 4 cm, and mass flow rate of 0.04 kg/s are presented in Table 2. It can be seen that with increasing the particle size, the performance indices of solar still decrease insignificantly (less than 0.1%). This reveals that the heat transfer coefficient of nanofluids with a smaller size of nanoparticles is higher (when nanoparticles with a diameter of 7nm are compared to the particles with a size of 100 nm); because the effective thermal conductivity of nanofluids containing smaller particles is greater.

5. Conclusion

The present paper, for the first time, investigates both experimentally and theoretically the effects of nanoparticle suspensions on the performance of a solar still equipped with a heat exchanger. The results were presented for laminar flow inside the heat exchanger and two types of nanofluids including SiO_2/water and Cu/water nanofluids. Effects of water depth in the basin, the mass flow rate in the heat exchanger, nanofluid type and concentration, nanoparticle size, and inlet temperature to heat exchanger on the yield, energy efficiency, and exergy efficiency have been investigated. The main findings of the study can be summarized as follows:

- Experiments revealed that the effects of weather conditions especially solar radiation on the performance indices of solar still are much higher than the effects of nanoparticle suspensions type.
- Microscopic and nanoscopic phenomenon occurring inside the heat exchanger including migration of nanoparticles, the wettability of nanofluid droplets, thermophoresis and diffusiophoresis, as well as aggregation and Brownian motion of nanoparticles affect the evaporation rate in the solar still.
- Using the heat exchanger inside solar still is not advantageous for inlet temperature < 50^{o}C. On the other hand, the yield of solar still can be increased more than two times, as compared to the solar still without the heat exchanger, when the inlet temperature is 70 ^{o}C.
- At high temperatures, using SiO_2/water instead of water provides more enhancement in evaporation rate while at low temperatures, Cu/water yields the maximum enhancement in evaporation rate.
- With decreasing the inlet temperature of the heat exchanger, the enhancement rate caused by nanofluids increases. However, using the heat exchanger in such conditions leads to a decrease in evaporation rate inside the solar still, resulting in a reduced performance

indices. For example, at an inlet temperature of 39 ^{o}C, the yield, thermal efficiency, and exergy efficiency of the solar still can be enhanced, respectively, by 9.86, 9.91, and 11.8 % by using Cu/water nanofluids at a concentration of 4%, but in this case, the amount of evaporation is negligible.

- At low inlet temperatures e.g. less than 50^{o}C, using Cu/water nanofluids is more effective than SiO_2/water nanofluids for evaporation rate enhancement in the solar still.
- At high inlet temperatures, i.e., 70 ^{o}C, despite having higher effective thermal conductivity, Cu/water nanofluids provide lower evaporation rate enhancement than that of SiO_2/water nanofluids.
- At the high inlet temperature of 70 ^{o}C, the maximum enhancement in evaporation rate is obtained by using SiO_2/water nanofluid with a volume fraction of 4%. However, the amount of enhancement is only about 1%, although the enhancement in convection heat transfer coefficient is not ignorable (by 15.4%).
- Using nanoparticles with a smaller size (7 nm instead of 100 nm) improves the performance indices of solar still less than 0.1% that is negligible.
-

Acknowledgment

The first author would like to thank the financial support provided by King Mongkut's University of Technology Thonburi, Thailand, for the research. The fifth author acknowledges the support provided by the Deanship of Research at King Fahd University of Petroleum and Minerals (KFUPM), Dhahran, Saudi Arabia, for this work under Research Grant RG1334.The sixth author acknowledges the support provided by the "Research Chair Grant" National Science and Technology Development Agency (NSTDA), the Thailand Research Fund (TRF), the National Research University Project (NRU) and King Mongkut's University of Technology Thonburi through the "KMUTT 55th Anniversary Commemorative Fund". The authors also would like to appreciate Professor Soteris Kalogirou at the Cyprus University of Technology, Cyprus for valuable help to improve the paper quality. Finally, the authors would like acknowledge FUTURE lab members in department of mechanical engineering, King Mongkut's University of Technology Thonburi for their valuable help during the project.

Appendix A. Solar radiation estimation on tilted surfaces

Solar radiation has been measured on a horizontal surface. To calculate the efficiency of the solar still, it is necessary to know the value of solar radiation on the tilted surfaces of solar still glass cover and the two solar collectors. In the following, the method of solar radiation estimation on tilted surfaces is given [28, 45, and 46]. The global radiation on a horizontal surface is the summation of diffuse and beam radiations. The ratio of diffuse radiation to the global radiation for a horizontal surface can be estimated as:

$$\frac{H_d}{H}=\begin{cases}1-0.249K_T & K_T<0.35\\ 1.557-1.84K_T & 0.35\le K_T\le 0.75\\ 0.177 & 0.75<K_T\end{cases} \quad (A.1)$$

In the above, H (W/m^2) is the global solar radiation on a horizontal surface which was measured by the pyranometer. The coefficient K_T is written as:

$$K_T=\frac{H}{H_o} \quad (A.2)$$

in which H_o is the amount of radiation outside of the atmosphere and is defined as:

$$H_o=I_{SC}\left(1+0.033\cos\frac{360n}{365}\right)\sin\alpha_s \quad (A.3)$$

where I_{SC} is the solar constant and equal to 1366.1 W/m^2, n is the day number (in the first day of January the value of n is 1) and α_s is the solar altitude angle. After obtaining diffuse radiation from the above, the amount of beam radiation can be obtained as:

$$H_b=H-H_d \quad (A.4)$$

Now, we have all the components of radiation on the horizontal surface, so the solar radiation intensity (I) on a tilted surface with slope of β can be estimated as:

$$I=H_bR_b+H_d\cos^2\frac{\beta}{2}+H\rho_r\sin^2\frac{\beta}{2} \quad (A.5)$$

in the above, ρ_r is ground albedo and is assumed to be 0.2. In addition, R_b is a geometric factor which is a function of day number, local time as well as latitude and longitude of test location. For more details, the readers can refer to Refs. [28] and [46].

Appendix B. Supplementary materials

Figures S1-S5 which have been discussed already in the text can be found in the online version of the article as supplementary materials.

References

[1] Z.L. Wang, J. Song, Piezoelectric nanogenerators based on zinc oxide nanowire arrays, Science 312 (2006) 242-246.

[2] X. Wang, J. Song, J. Liu, Z. L. Wang, Direct-current nanogenerator driven by ultrasonic waves, Science 316 (2007)102-105.

[3] R. Sood, S. Cavaliere, D. J. Jones, J. Rozière, Electrospun nanofibre composite polymer electrolyte fuel cell and electrolysis membranes, Nano Energy 26(2016) 729-745.

[4] X. Zuo, J. Zhu, P. M. Buschbaum, Y. J. Cheng, Silicon based lithium-ion battery anodes: A chronicle perspective review, Nano Energy 31(2017) 113-143.

[5] J. K. Sun, Y. Jiang, X. Zhong, J. S. Hu, L.J. Wan, Three-dimensional nanostructured electrodes for efficient quantum-dot-sensitized solar cells, Nano Energy 32(2017)130-156.

[6] S.U.S. Choi, Enhancing thermal conductivity of fluids with nanoparticles, in developments and applications of Non-Newtonian flows, ASME FED 231/MD, 66(1995) 99–103.

[7] J. Navas, A. S. C., E. I. Martín, M. Teruel, J. J. Gallardo, T. Aguilar, R. G. Villarejo, R. Alcántara, C. F. Lorenzo, J. C. Piñero, J. M. Calleja, On the enhancement of heat transfer fluid for concentrating solar power using Cu and Ni nanofluids: An experimental and molecular dynamics study, Nano Energy 27(2016) 213-224.

[8] G. Ni, N. Miljkovic, H. Ghasemi, X. Huang, S. V. Boriskina, C. T. Lin, J. Wang, Y. Xu, Md. M. Rahman, T. Zhang, G. Chen, Volumetric solar heating of nanofluids for direct vapor generation, Nano Energy 17(2015) 290-301.

[9] H. Jin, G. Lin, L. Bai, A. Zeiny, D. Wen, Steam generation in a nanoparticle-based solar receiver, Nano Energy 28(2016) 397-406.

[10] M. Milanese, G. Colangelo, F. Iacobazzi, A. de Risi, Modeling of double-loop fluidized bed solar reactor for efficient thermochemical fuel production, Sol. Energy Mater. Sol. Cells 160 (2017) 174-181.

[11] O. Mahian, A. Kianifar, S. A. Kalogirou, I. Pop, S. Wongwises, A review of the applications of nanofluids in solar energy, Int. J. Heat Mass Transf. 57(2013) 582-594.

[12] O. Mahian, A. Kianifar, A.Z. Sahin, S. Wongwises, Entropy generation during Al_2O_3/water nanofluid flow in a solar collector: effects of tube roughness, nanoparticle size, and different thermophysical models, Int. J. Heat Mass Transf. 78(2014) 64-75.

[13] O. Mahian, A. Kianifar, A.Z. Sahin, S. Wongwises, Performance analysis of a minichannel-based solar collector using different nanofluids, Energy Convers. Manag. 88(2014)129-138.

[14] J. B. Puga, B. D. Bordalo, D. J. Silva, M. M. Dias, J. H. Belo, J. P. Araújo, J. C.R.E. Oliveira, A. M. Pereira, J. Ventura, Novel thermal switch based on magnetic nanofluids with remote activation, Nano Energy 31 (2017) 278-285.

[15] P. Nitiapiruk, O. Mahian, A. S. Dalkilic, S. Wongwises, Performance characteristics of a microchannel heat sink using TiO_2/water nanofluid and different thermophysical models, Int. Communications Heat Mass Transf. 47(2013) 98-104.

[16] A. Celen, A. Çebi, M. Aktas, O. Mahian, A. S. Dalkilic, S. Wongwises, A review of nanorefrigerants: Flow characteristics and applications, Int. J. Refrigeration 44(2014) 125-140.

[17] R. Saidur, K.Y. Leong, H.A. Mohammad, A review on applications and challenges of nanofluids, Renew. Sustainable Energy Reviews 15 (2011)1646-1668.

[18] M.K. Gnanadason, P.S. Kumar, S. Rajakumar, M.H.S. Yousuf, Effect of nanofluids in a vacuum single basin solar still, I.J.AERS 1(2011) 171–177.

[19] A.E. Kabeel, Z.M. Omara, F.A. Essa, Improving the performance of solar still by using nanofluids and providing vacuum, Energy Convers. Manag. 86(2014) 268-274.

[20] A.E. Kabeel, Z.M. Omara, F.A. Essa, Enhancement of modified solar still integrated with external condenser using nanofluids: An experimental approach, Energy Convers. Manag. 78(2014) 493-498.

[21] Z.M. Omara, A.E. Kabeel, F.A. Essa, Effect of using nanofluids and providing vacuum on the yield of corrugated wick solar still, Energy Convers. Manag. 103(2015) 965-972.

[22] T. Elango, A. Kannan, K. K. Murugavel, Performance study on single basin single slope solar still with different water nanofluids, Desalination 360(2015) 45-51.

[23] L. Sahota, G.N. Tiwari, Effect of Al_2O_3 nanoparticles on the performance of passive double slope solar still, Sol. Energy 130(2016) 260-272.

[24] L. Sahota, G.N. Tiwari, Effect of nanofluids on the performance of passive double slope solar still: A comparative study using characteristic curve, Desalination 388(2016) 9-21.

[25] S.W. Sharshir, G. Peng, L. Wu, N. Yang, F.A. Essa, A.H. Elsheikh, S. I.T. Mohamed, A.E. Kabeel, Enhancing the solar still performance using nanofluids and glass cover cooling: Experimental study, Appl. Therm. Eng. 113(2017) 684-693.

[26] Y. Ding, H. Alias, D. Wen, R.A. Williams, Heat transfer of aqueous suspensions of carbon nanotubes (CNT nanofluids), Int. J. Heat Mass Transf. 49(2006) 240-250.

[27] H. Xie, Y. Li, W. Yu, Intriguingly high convective heat transfer enhancement of nanofluid coolants in laminar flows, Phys. Lett. A: Gen., Atomic Solid State Phys. 374(2010) 2566-2568.

[28] J. A. Duffie, W. A. Beckman, Solar engineering of thermal processes, 2nd ed., 919. New York: John Wiley & Sons, 1991.

[29] A. K. Tiwari and G. N. Tiwari, Solar Distillation Practice for Water Desalination Systems, Anshan Publishers, India, 2008.

[30] R. Dunkle, Solar water distillation, The roof type still and a multiple effect diffusion still, in: Internat, Developments in Heat Transfer, ASME, Proc. Internat. Heat Transfer, Part V, University of Colorado, 1961, 895.

[31] R.V. Dunkl, CSIRO, Solar Water Distillation: The Roof Type Still and a Multiple Effect Diffusion Still, CSIRO, New York, NY, 1961.

[32] F.P. Incropera, D.P. DeWitt, Introduction to Heat Transfer, 3rd edition, John Wiley & Sons, Inc., New York, USA, 1996.

[33] K.V. Sharma, P.K. Sarma, W.H. Azmi, R. Mamat, K. Kadirgama, Correlations to predict friction and forced convection heat transfer coefficients of water based nanofluids for turbulent flow in a tube, Int. J. Microscale Nanoscale Therm, Fluid Transp. Phenom. 3(2012) 1–25.

[34] J. Fernandez, N. Chargoy, Multi-stage, indirectly heated solar still, Sol. Energy 44(1990) 215-223.

[35] A. Kianifar, S.Z. Heris, O. Mahian, Exergy and economic analysis of a pyramid-shaped solar water purification system: active and passive cases, Energy 38 (2012) 31-36.

[36] N. Rahbar, J.A. Esfahani, Productivity estimation of a single-slope solar still: Theoretical and numerical analysis, Energy 49 (2013) 289-297.

[37] S.Z. Heris, S.G. Etemad, M.N. Esfahany, Convective heat transfer of a Cu/Water nanofluid flowing through a circular tube, Exp. Heat Transf. 22(2009) 217-227.

[38] B. Xiao, Y. Yangc, L. Chen, Developing a novel form of thermal conductivity of nanofluids with Brownian motion effect by means of fractal geometry, Powder Technology 239(2013) 409–414.

[39] Y. He, Y. Jin, H. Chen, Y. Ding, D. Cang, H. Lu, Heat transfer and flow behaviour of aqueous suspensions of TiO_2 nanoparticles (nanofluids) flowing upward through a vertical pipe. Int. J. Heat Mass Transf. 50(2007) 2272-2281.

[40] D. Gloss, H. Herwig, Wall roughness effects in laminar flows: an often ignored though significant issue, Exp. Fluids 49(2010) 461–470.

[41] R. N. Wenzel, Resistance of solid surfaces to wetting by water, Ind. Eng. Chem. Res. 28(1936) 988.

[42] K.S. Hong, T.K. Hong, H.S. Yang, Thermal conductivity of Fe nanofluids depending on the cluster size of nanoparticles, Appl. Phys. Lett. 88(2006) 1-3.

[43] W. Wei, J. Cai, X. Hu, Q. Han, S. Liu, Y. Zhou, Fractal analysis of the effect of particle aggregation distribution on thermal conductivity of nanofluids, Phys. Lett. A 380(2016)2953-2956.

[44] J. Cai, X. Hu, B. Xiao, Y. Zhou, W. Wei, Recent developments on fractal-based approaches to nanofluids and nanoparticle aggregation, Int. J. Heat Mass Transf. 105(2017) 623-637.

[45] J. F. Orgill, K. G. T. Hollands, Correlation equation for hourly diffuse radiation on a horizontal surface. Sol. Energy 19(1977) 357–359.

[46] R. Foster, M. Ghassemi, A. Cota, Solar Energy: renewable Energy and the Environment, CRC Press, 2010.

Vitae

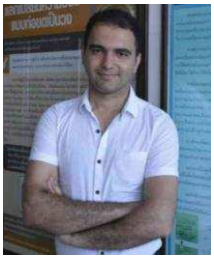

Omid Mahian received his Ph.D. degree in Mechanical Engineering, from Ferdowsi University of Mashhad, Iran. He is currently a research associate at King Mongkut's University of Technology Thonburi, Thailand. His research interests are nanofluids, heat transfer, solar energy, entropy generation minimization, and exergy analysis of energy systems. He has more than 75 papers in archival journals, two book chapters, and has served as reviewer and editor for more than 70 international journals. He is currently an associate editor of Journal of Thermal Analysis and Calorimetry published by Springer.

Ali Kianifar is a professor in the Department of Mechanical Engineering, Ferdowsi University of Mashhad, Iran. He received his B.Sc. (Hons), M.Sc., and Ph.D. from London University, Bath University, and Strathclyde University, respectively. He has been teaching and researching at Ferdowsi University since 1989. His main research interests are Renewable energy and energy recovery. He has published two books, two book chapters and 80 articles in journals and proceedings and carried out more than 15 national research projects.

Saeed Zeinali Heris is a Professor at the University of Tabriz. He takes his Ph.D. in Chemical Engineering from Isfahan University of Technology in 2006. He worked on heat transfer performance of nanofluid as Ph.D. thesis. His research interests are non-Newtonian flow and heat transfer, energy system, heat transfer enhancement, thermosiphon and nanofluid.

He has published more than 100 articles in well-recognized journals and proceedings. He published one book titled nanofluids and one book chapter in CRC Concise Encyclopedia of Nanotechnology.

Dongsheng Wen is a Chair Professor in the School of Chemical and Process Engineering at the University of Leeds. He received his DPhil from the University of Oxford, and is the Fellow of Royal Society of Chemistry (FRSC), Energy Institute (FEI), and Institute of Nanotechnology (FION), a Chartered Engineer (CEng) and a Chartered Scientist (CSci). He has published 150 papers in peer-reviewed journals, which is well received in the community (i.e. total citation >4500, and current H-index-28). His research covers a wide spectrum of nanotechnology and engineering science, and is a leading expert in engineering nanomaterials for energy applications.

Ahmet Z. Sahin is a Professor of Mechanical Engineering at King Fahd University of Petroleum and Minerals (KFUPM), Dhahran, Saudi Arabia. He received his Ph.D. in Mechanical Engineering from the University of Michigan, Ann Arbor, MI, USA in 1988. He has published over 250 technical Journal/Conference papers. He received the KFUPM Distinguished Researcher Award three times; in 2000, 2005, and 2010, respectively. His research interests include Thermodynamic design optimization, Entropy generation minimization, Renewable energy, solar energy, and wind energy applications.

Somchai Wongwises is currently a Professor of Mechanical Engineering, Faculty of Engineering at King Mongkut's University of Technology Thonburi, Bangmod, Thailand. He received his Doktor Ingenieur (Dr.-Ing.) in Mechanical Engineering from the University of Hannover, Germany, in 1994. He has published more than 370 articles in archival journals and international conferences. His research interests include Gas-Liquid Two-Phase Flow, Heat Transfer Enhancement, and Thermal System Design. Professor Wongwises is the head of the Fluid Mechanics, Thermal Engineering, and Multiphase Flow Research Laboratory (FUTURE).

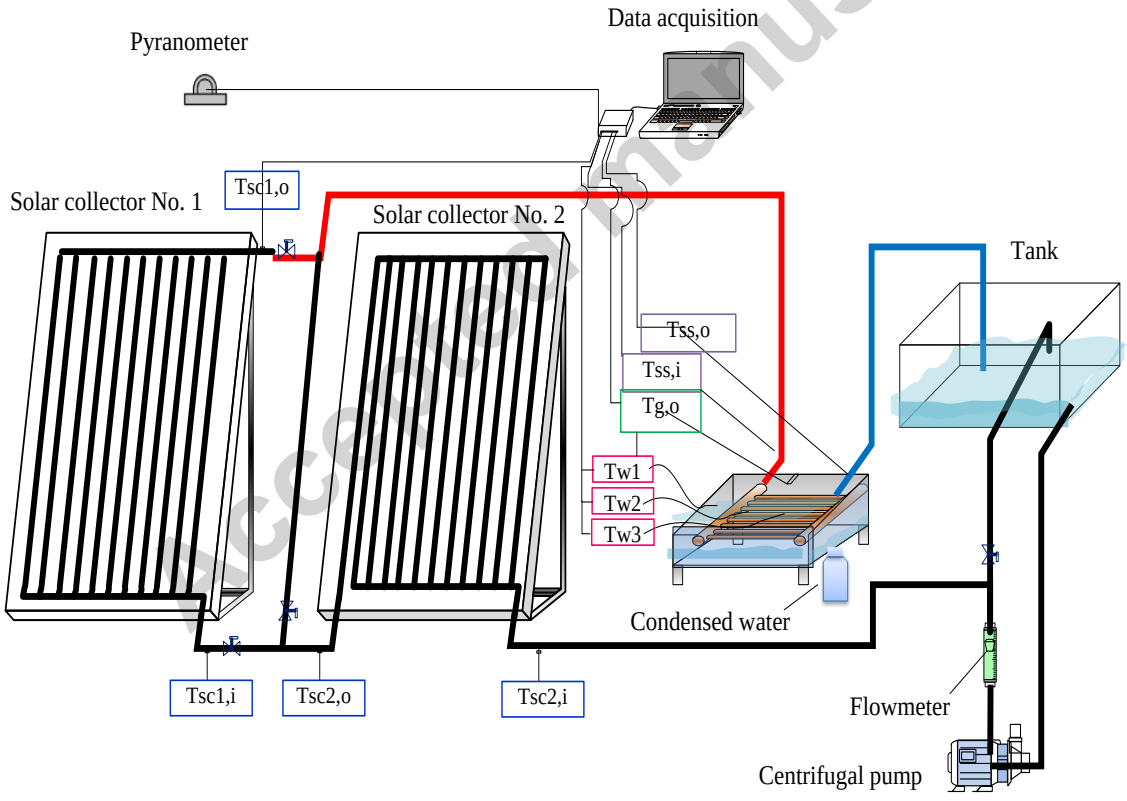

Fig. 1. Schematic of the experimental set-up

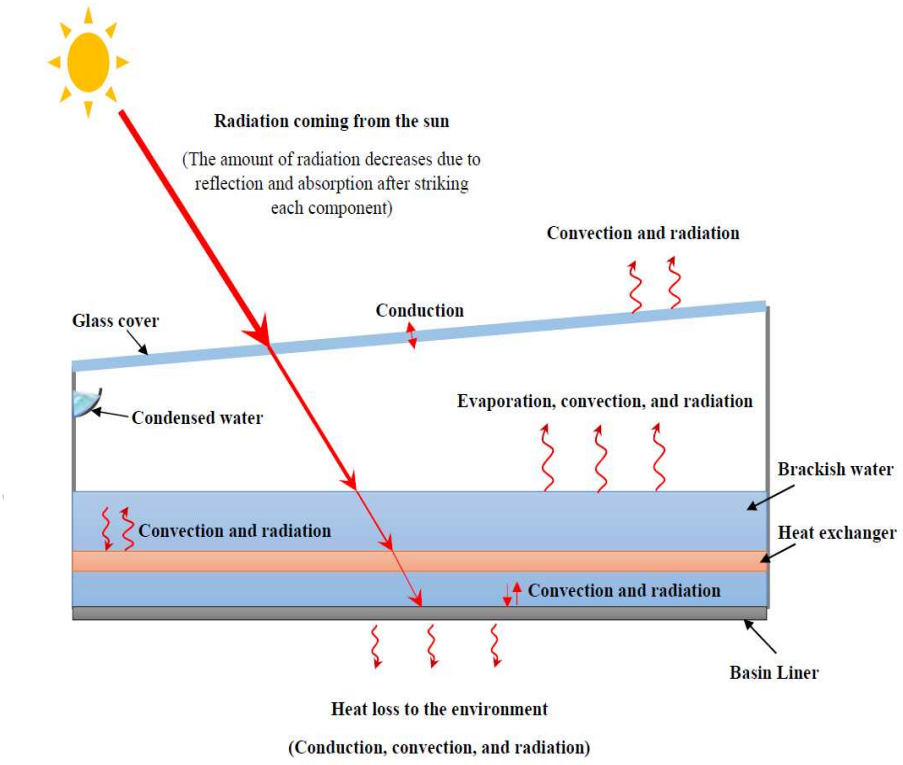

a)

b)

Fig. 2. (a) Heat transfer modes considered in modeling of the solar still, (b) top view of the solar still.

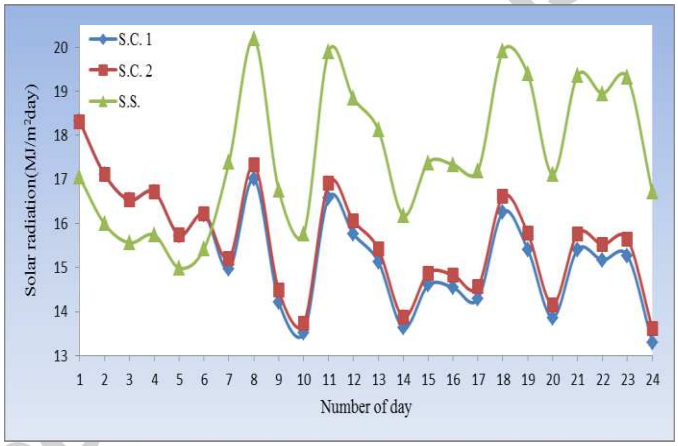

Fig. 3. Total solar radiation on solar still (S.S.) and two solar collectors during 24 selected days

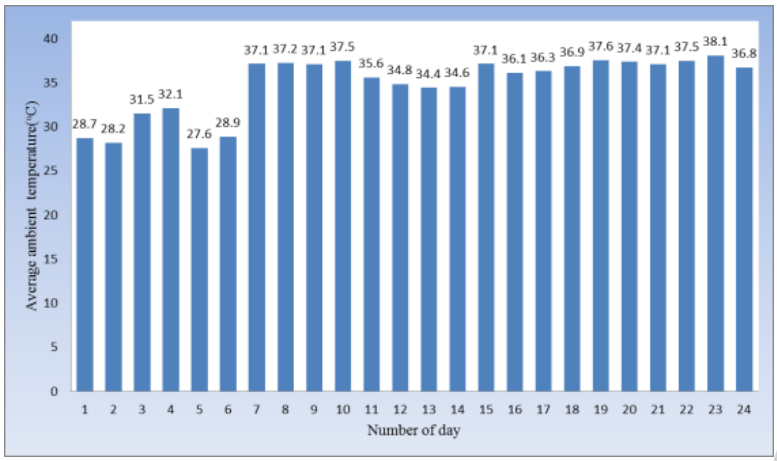

Fig. 4. Average ambient temperature during each of the selected days

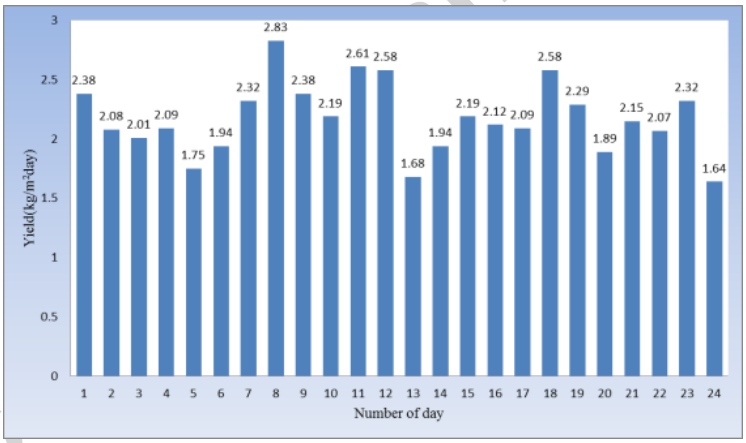

a)

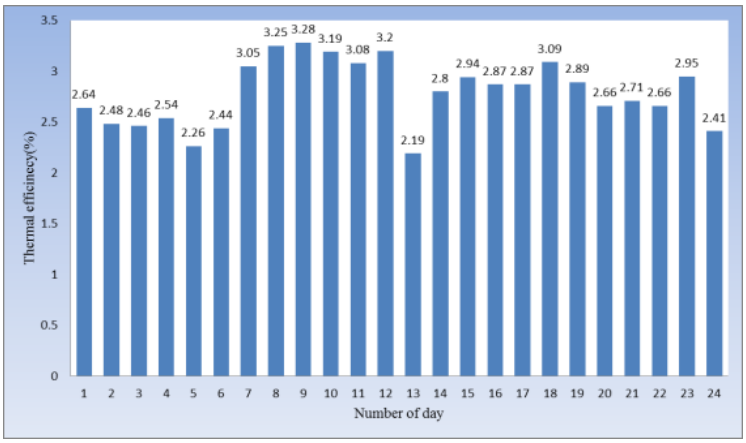

b)

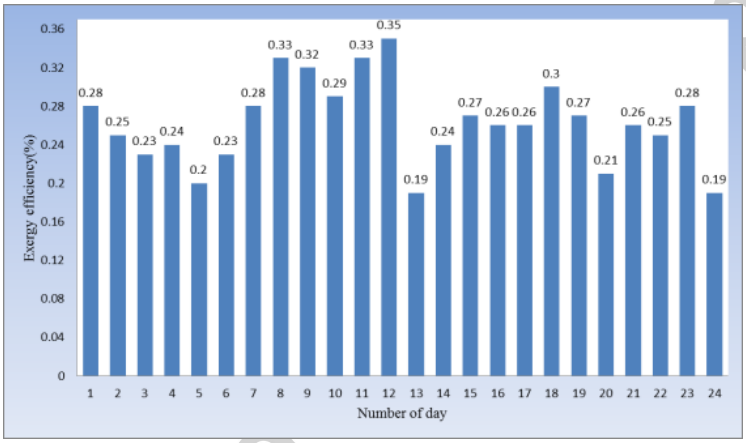

c)

Fig. 5. Experimental (a) yield, (b) thermal efficiency, (c) exergy efficiency during each of the selected days

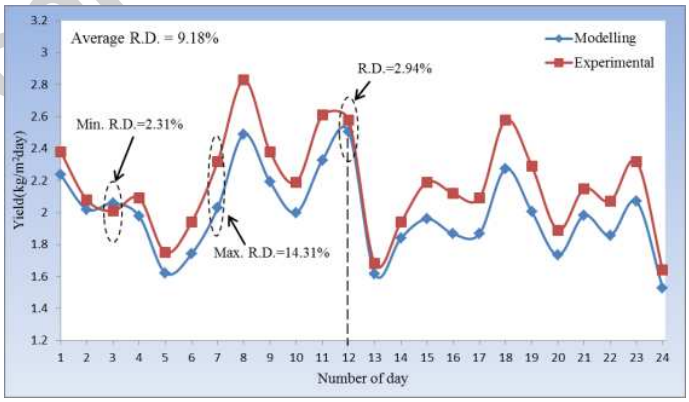

a)

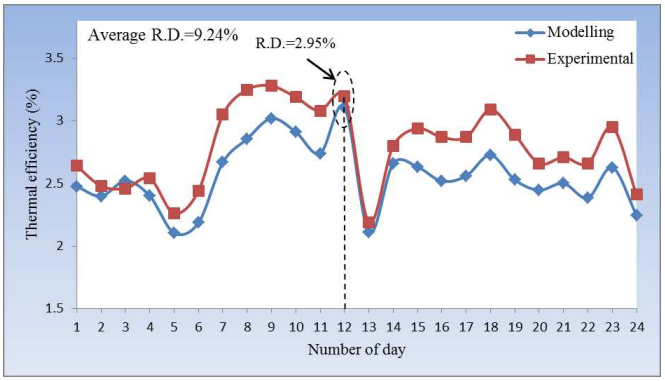

b)

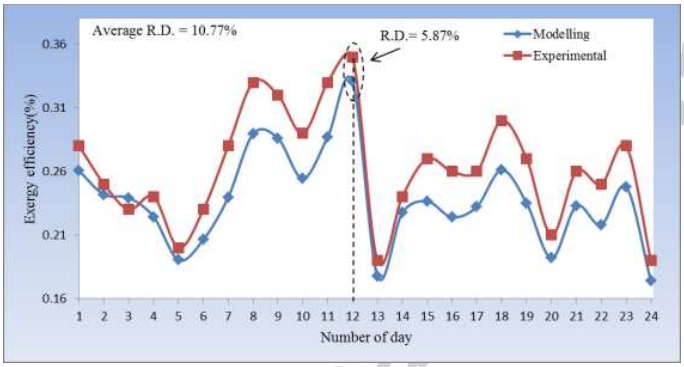

c)

Fig. 6. Comparison between experimental and numerical results for (a) yield (b) thermal efficiency (c) exergy efficiency during selected days

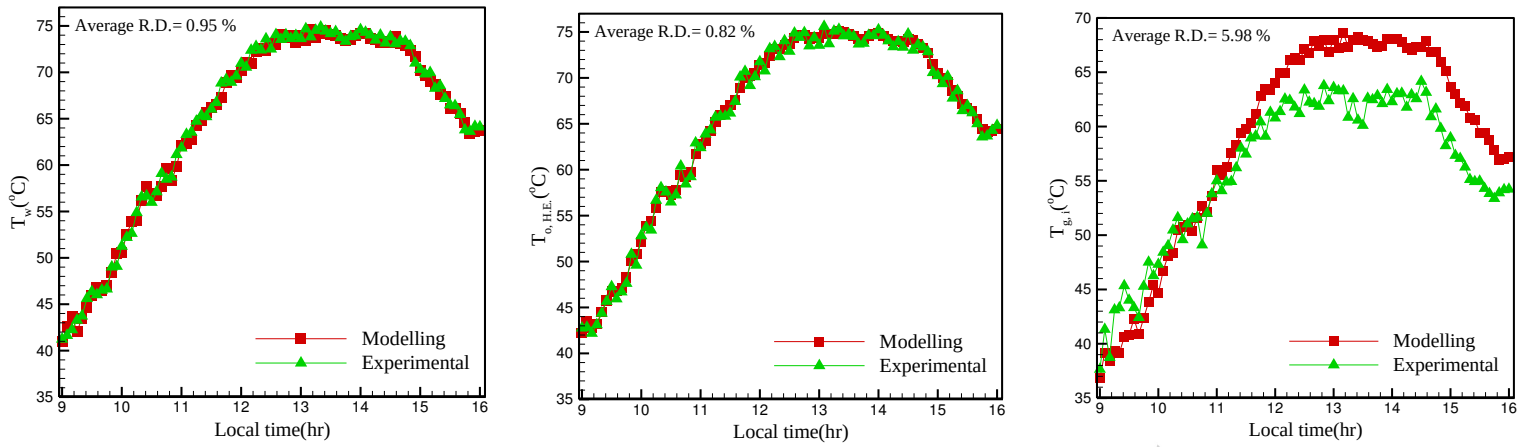

a) b) c)

Fig. 7. Comparison between experimental and numerical results for temperatures of (a) basin water (b) heat exchanger outlet (c) glass cover

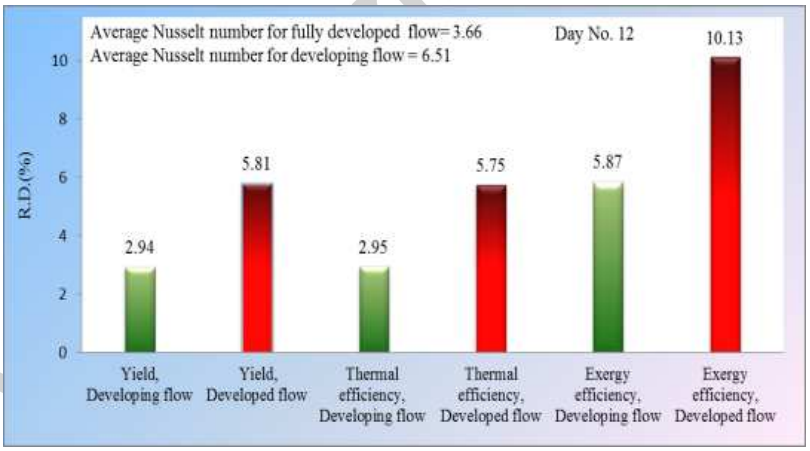

Fig. 8. Effect of average Nusselt number on ratio difference between experimental and numerical results

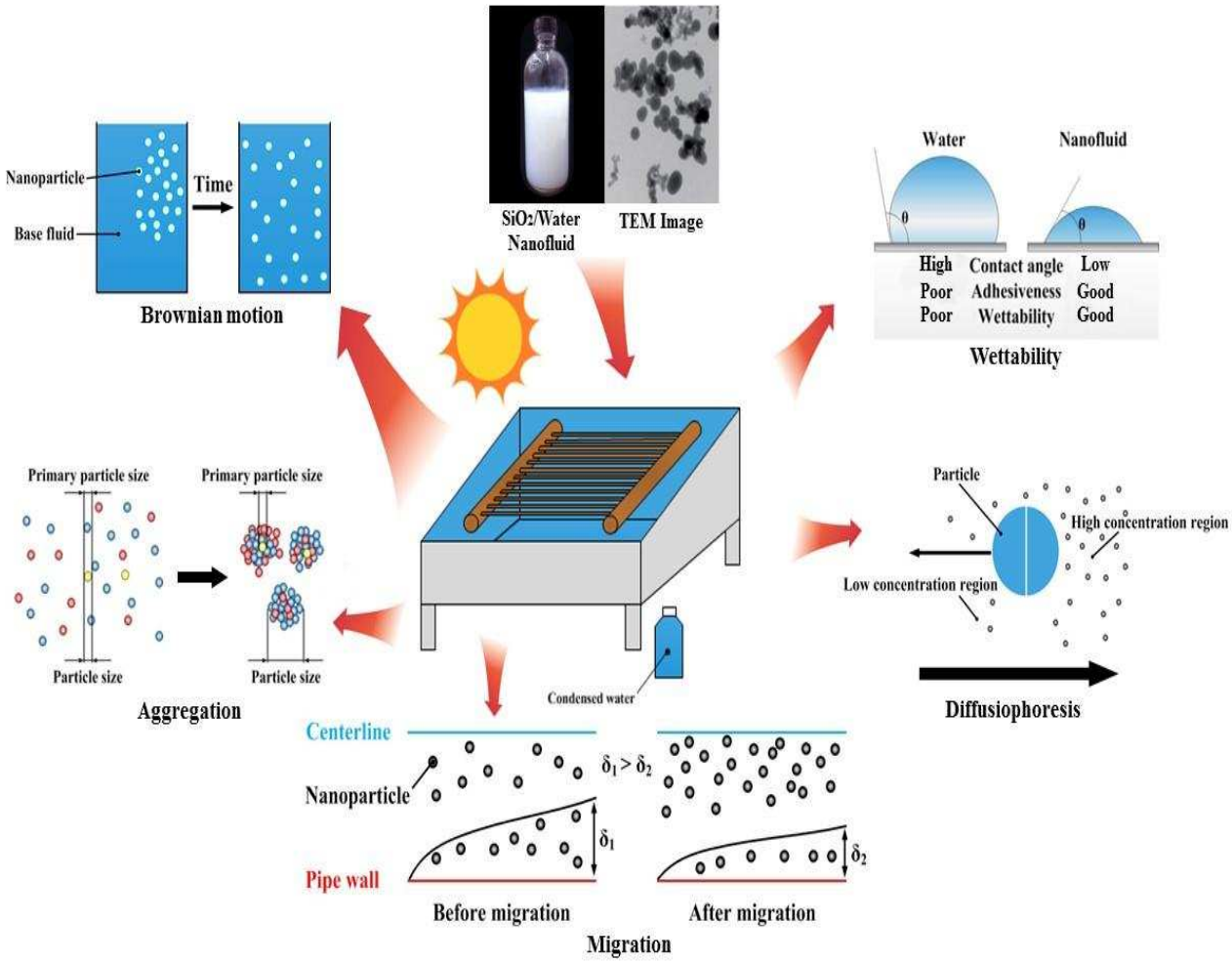

Fig. 9. A schematic of microscopic and nanoscopic phenomena occurring inside heat exchanger affecting the evaporation rate in the solar still

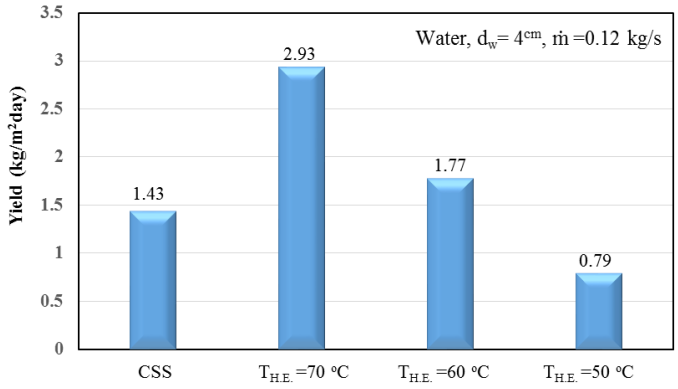

a)

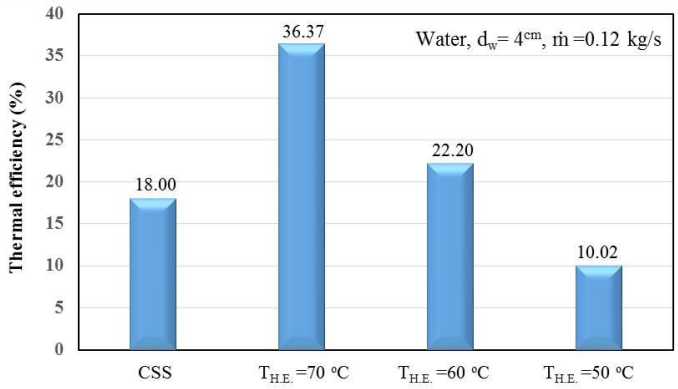

b)

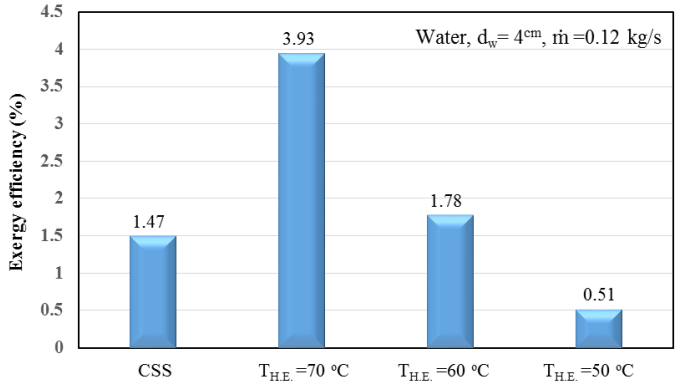

c)

Fig. 10. Comparison between the performance of solar stills with and without heat exchanger

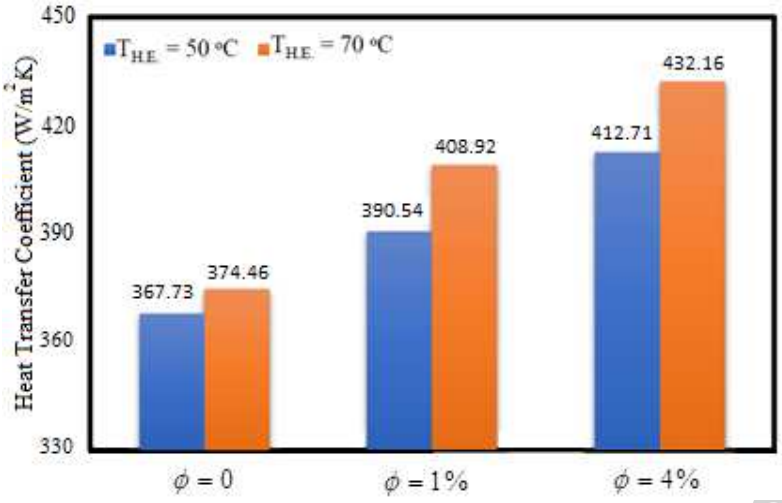

Fig. 11. Effect of nanofluid concentration and inlet temperature on convection heat transfer coefficient for SiO_2/water nanofluid at d_w = 4 cm and $\dot{m}$ = 0.04 kg/s.

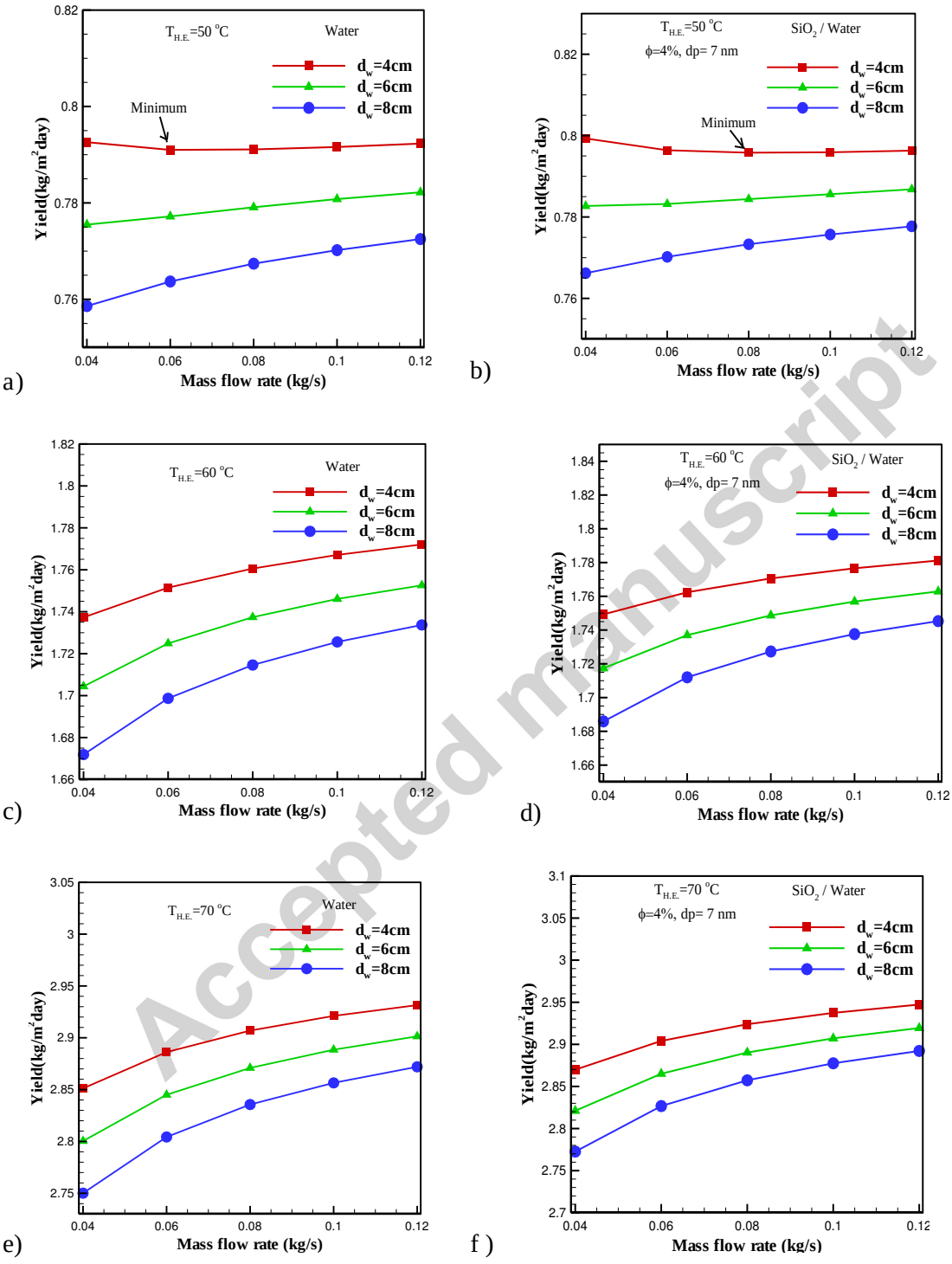

Fig. 12. Effects of water depth on solar still yield at different inlet temperatures of heat exchanger (Left hand: Water, Right hand: SiO_2/ water nanofluid with 4% volume concentration)

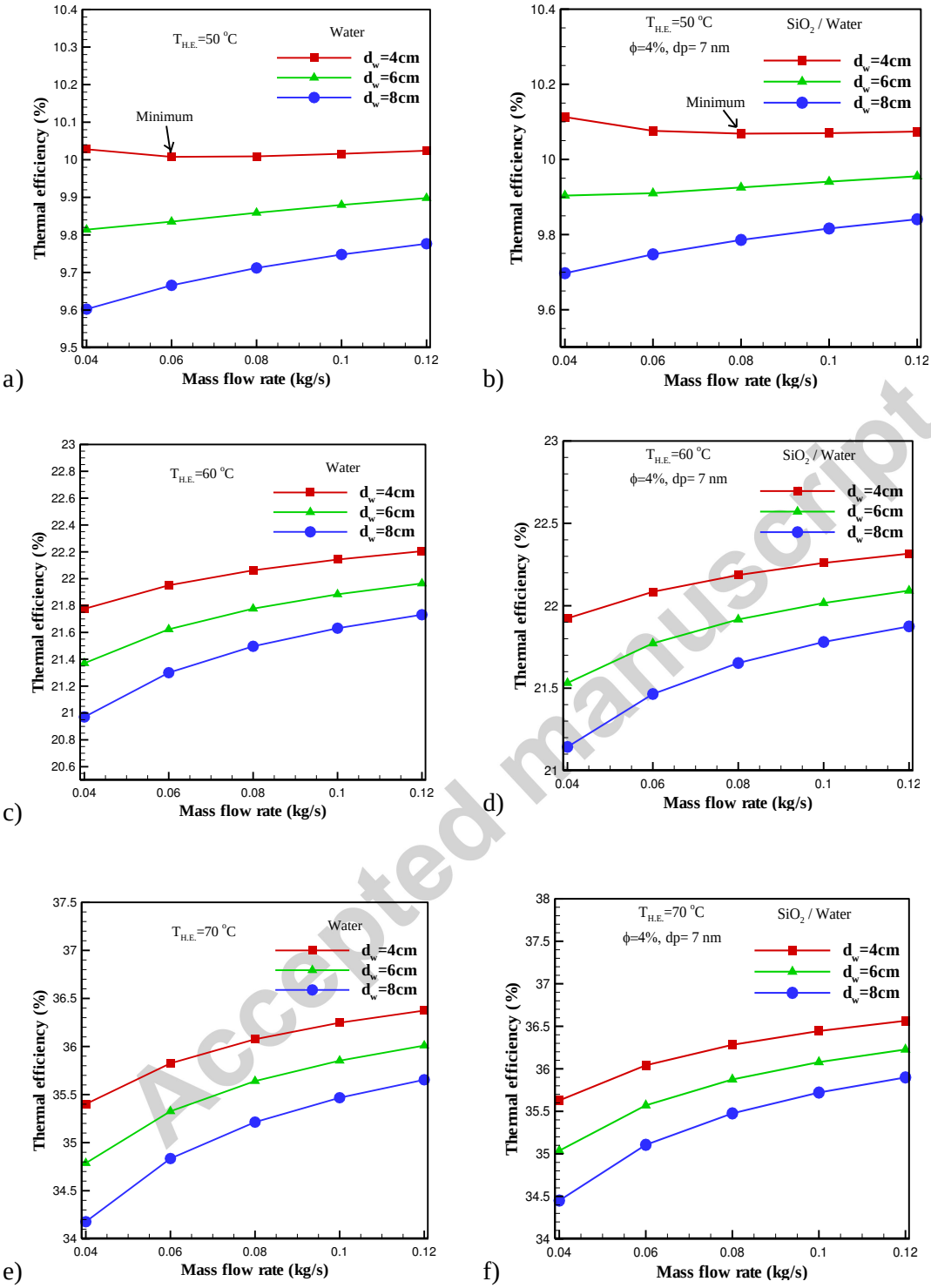

Fig. 13. Effects of water depth on solar still thermal efficiency at different inlet temperatures of heat exchanger (Left hand: Water, Right hand: SiO_2/ water nanofluid with 4% volume concentration)

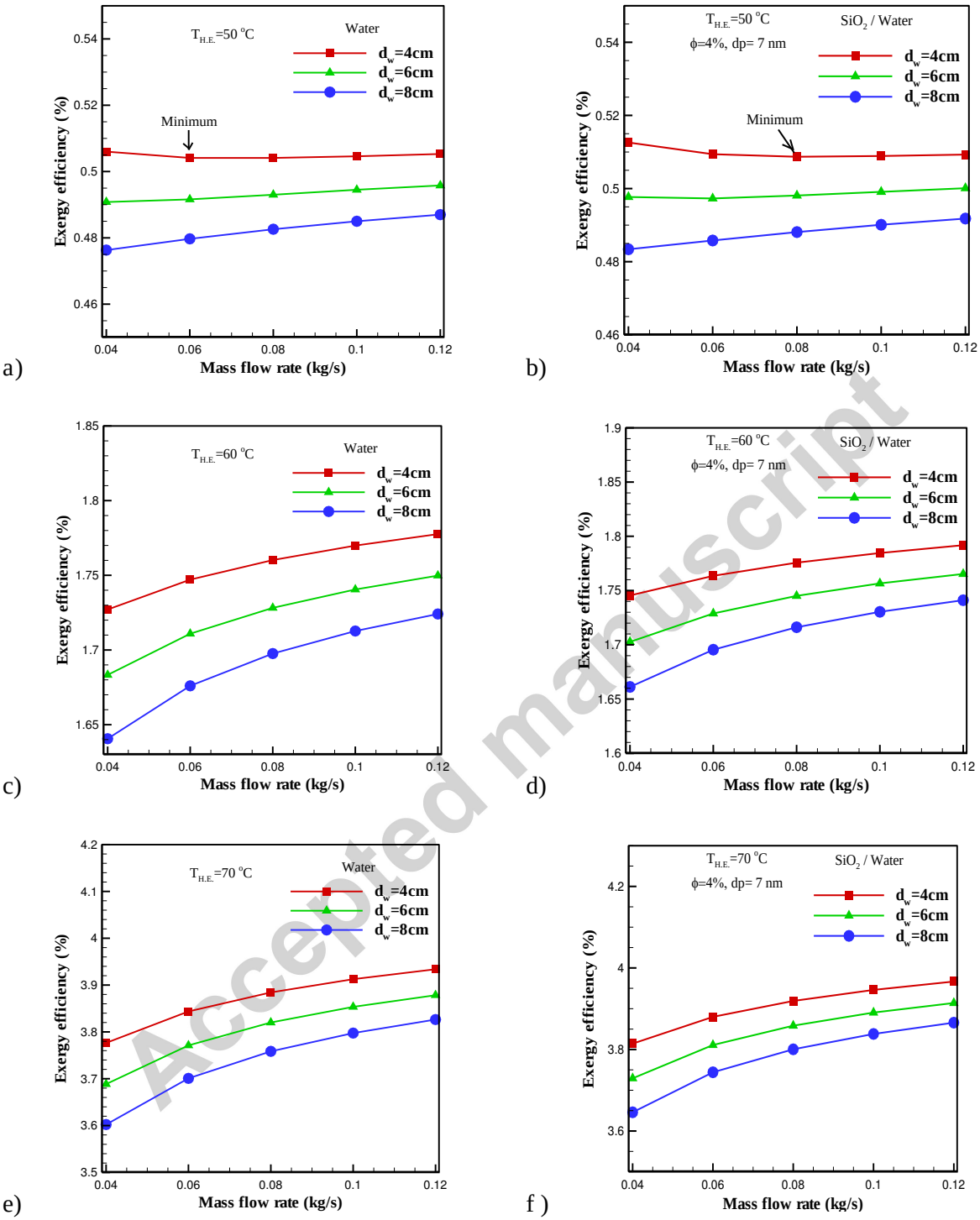

Fig. 14. Effects of water depth on solar still exergy efficiency at different inlet temperatures of heat exchanger (Left hand: Water, Right hand: SiO_2/ water nanofluid with 4% volume concentration)

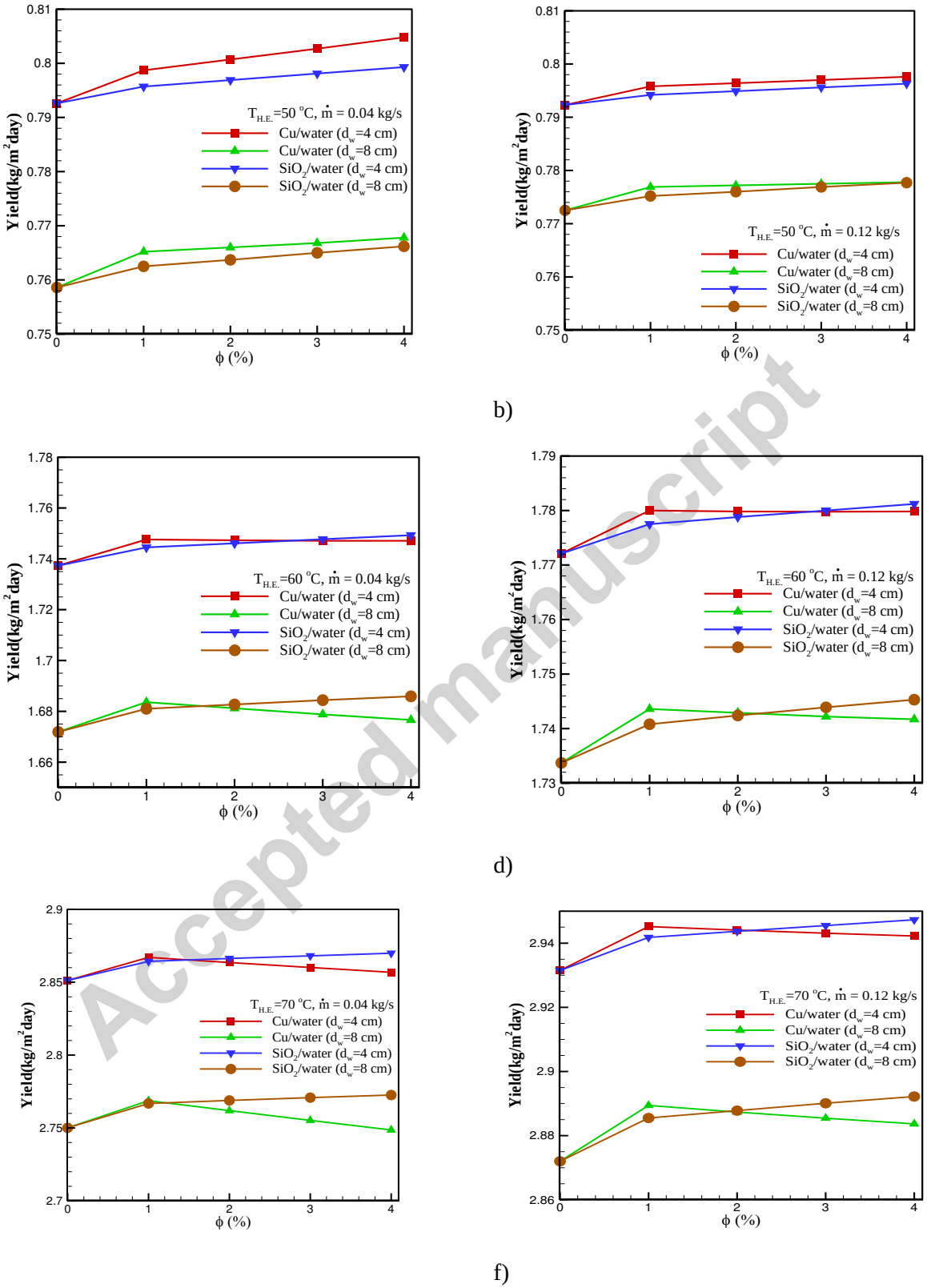

Fig. 15. Effects of using Cu/water and SiO_2/water nanofluids with varying concentrations on the yield of solar still

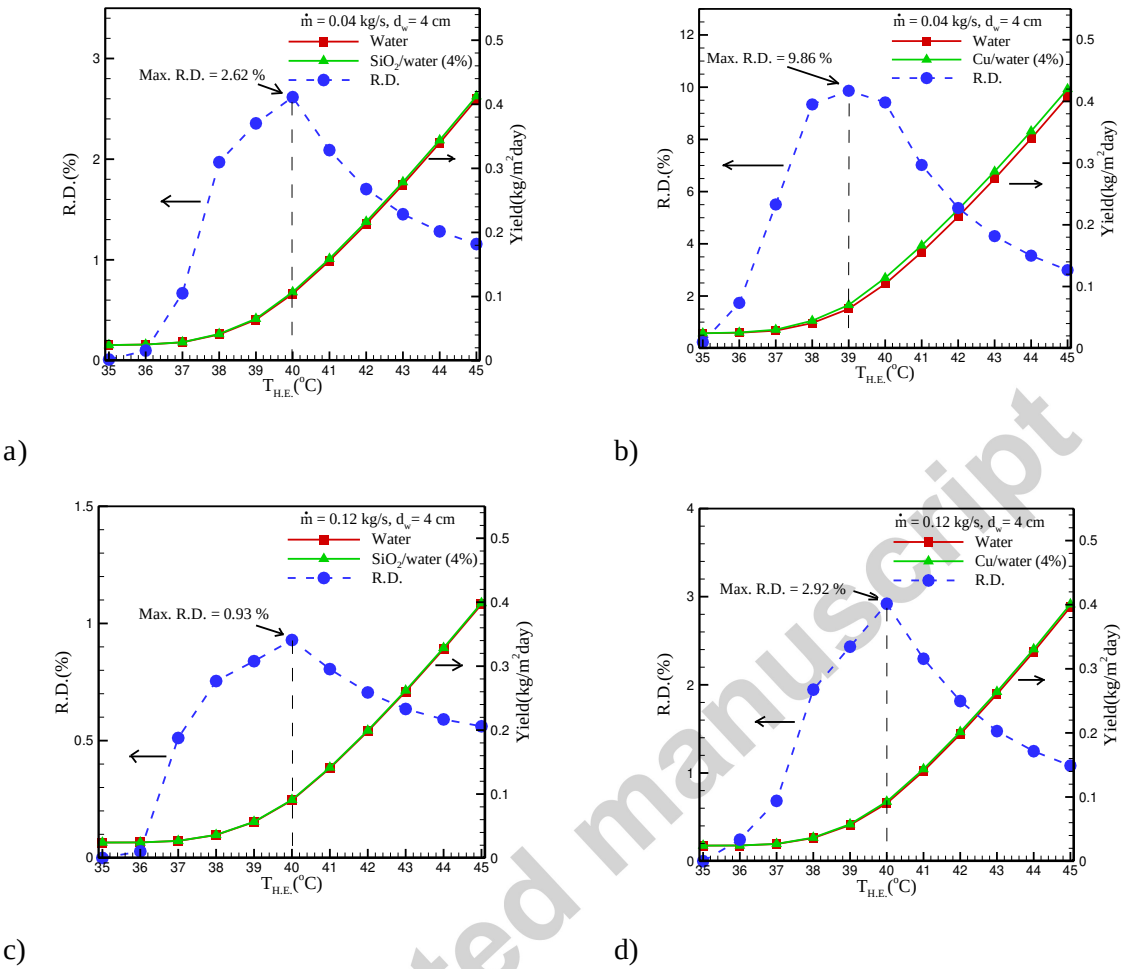

Fig. 16. Yield of solar still for inlet temperatures of 35 to 45 °C and different nanofluids.

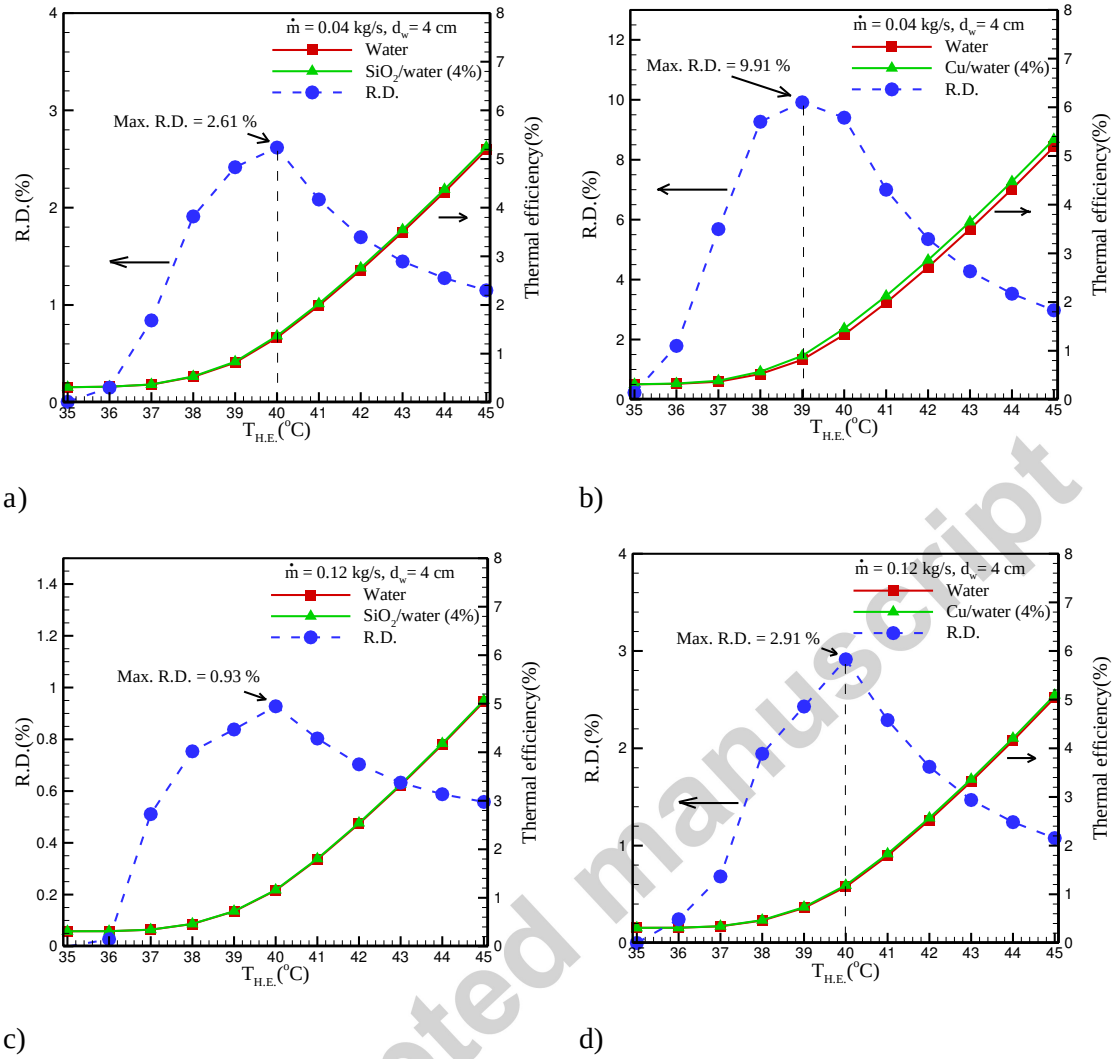

Fig. 17. Thermal efficiency of solar still for inlet temperatures of 35 to 45 °C and different nanofluids.

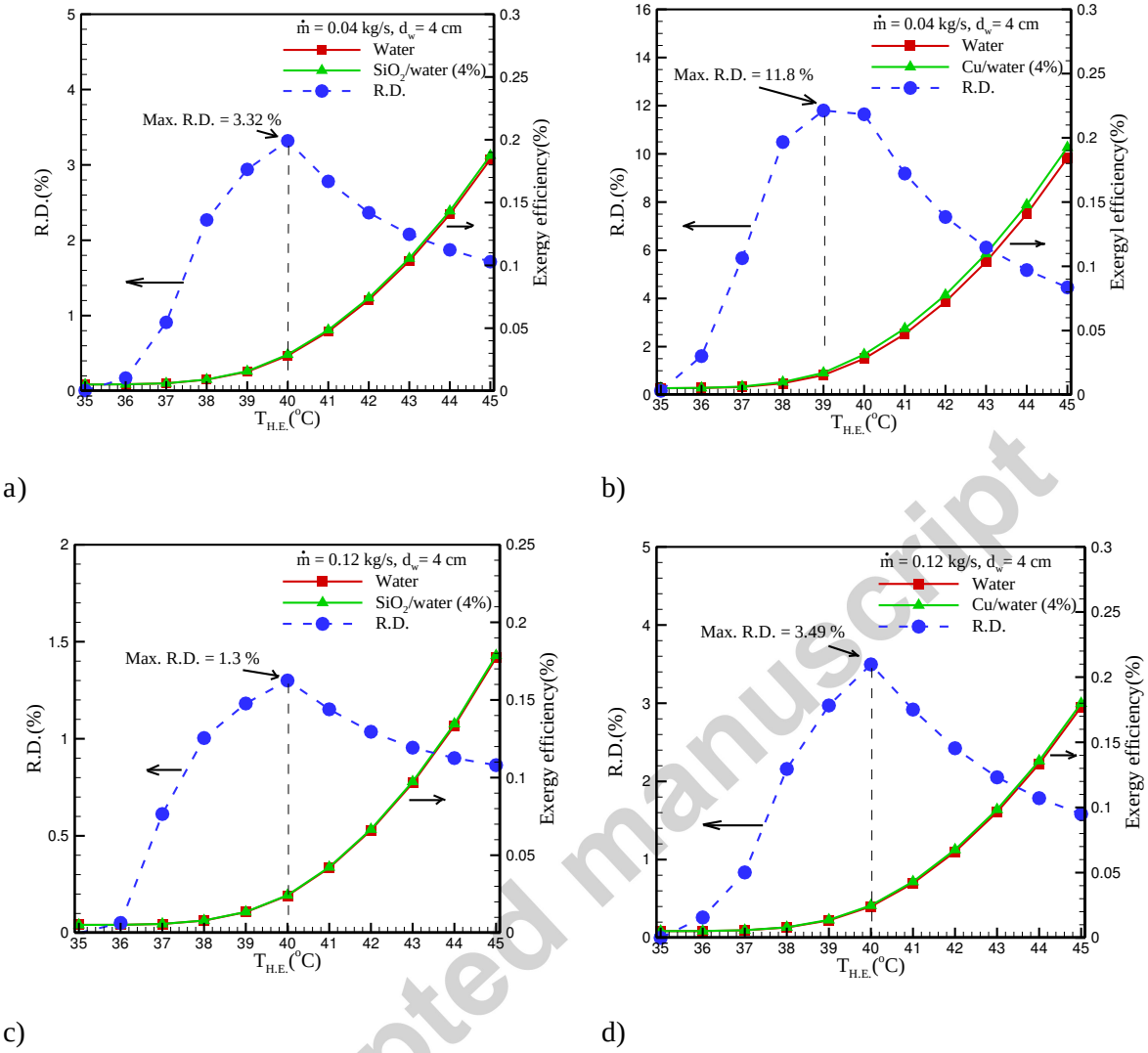

Fig. 18. Exergy efficiency of solar still for inlet temperatures of 35 to 45 °C and different nanofluids.

Table 1. Experimental conditions during 24 selected days.

Day No.	Working fluid (volume fraction %)	Volume flow rate (m^3/s)	Water depth (cm)	Nanoparticle size (nm)
1	Water	5×10^{-5}	4	-
2	Water	5×10^{-5}	8	-
3	Water	8.33×10^{-5}	4	-
4	Water	6.67×10^{-5}	4	-
5	Water	8.33×10^{-5}	8	-

6	Water	6.67×10^{-5}	8	-
7	Nanofluid (0.5)	5×10^{-5}	4	**7**
8	Nanofluid (0.5)	6.67×10^{-5}	4	**7**
9	Nanofluid (0.5)	8.33×10^{-5}	4	**7**
10	Nanofluid (0.5)	5×10^{-5}	8	**7**
11	Nanofluid (1)	6.67×10^{-5}	4	**7**
12	Nanofluid (1)	8.33×10^{-5}	4	**7**
13	Nanofluid (1)	5×10^{-5}	8	**7**
14	Nanofluid (1)	8.33×10^{-5}	8	**7**
15	Nanofluid (2)	5×10^{-5}	4	**7**
16	Nanofluid (2)	6.67×10^{-5}	4	**7**
17	Nanofluid (2)	8.33×10^{-5}	4	**7**
18	Nanofluid (2)	8.33×10^{-5}	8	**7**
19	Nanofluid (2)	5×10^{-5}	4	**40**
20	Nanofluid (2)	6.67×10^{-5}	4	**40**
21	Nanofluid (0.5)	5×10^{-5}	8	**7**
22	Nanofluid (2)	8.33×10^{-5}	8	**7**
23	Nanofluid (1)	8.33×10^{-5}	4	**40**
24	Nanofluid (2)	5×10^{-5}	4	**7**

Table 2. Effect of nanoparticles on the performance of solar still for inlet temperature of 70 ^{o}C.

Volume fraction (%)	**Yield (kg/m^{2}day)**			**(%) Thermal efficiency**			**(%) Exergy efficiency**		
	d_p=7nm	d_p=100 nm	R.D. (%)	d_p=7 nm	d_p=100 nm	R.D. (%)	d_p=7 nm	d_p=100 nm	**R.D. (%)**
1	2.8671	2.865	0.073	35.5935	35.5689	0.069	3.8087	3.8046	**0.107**

2	2.8635	2.8615	0.069	35.5508	35.5264	0.069	3.8023	3.7983	**0.105**
3	2.8601	2.8581	0.069	35.5097	35.4856	0.068	3.7963	3.7923	**0.105**
4	2.8568	2.8548	0.070	35.4696	35.4458	0.067	3.7904	3.7865	**0.103**

Highlights

- Performance of solar still equipped with heat exchanger using nanofluids tested
- Effect of inlet temperature to heat exchanger and various nanofluid samples modeled
- Using heat exchanger and nanofluids at low inlet temperatures is not beneficial
- At high inlet temperatures nanofluids effect on solar still yield is marginal (1%)
- A nanofluid with a higher effective thermal conductivity may be less efficient